Fall 2021

Biogeochemical Stressors and Ecological Response in Great Bay Estuary, NH/ME

Anna Lowien
University of New Hampshire, Durham

BIOGEOCHEMICAL STRESSORS AND ECOLOGICAL RESPONSE IN GREAT BAY ESTUARY, NH/ME

BY

ANNA E. LOWIEN

B.S. Environmental Science and Policy, University of Maryland, 2019

THESIS

Submitted to the University of New Hampshire

In Partial Fulfillment of

the Requirements for the Degree of

Master of Science

In

Natural Resources and the Environment: Ecosystem Science

September, 2021

BIOGEOCHEMICAL STRESSORS AND ECOLOGICAL RESPONSE IN GREAT BAY ESTUARY, NH/ME

BY

ANNA E. LOWIEN

This thesis was examined and approved in partial fulfillment of the requirements for the degree of Master of Science in Natural Resources: Ecosystem Science by:

Thesis Director, Dr. William H. McDowell, Professor

Natural Resources and the Environment

Dr. Kalle Matso, Research Project Manager,

Marine Sciences & Ocean Engineering

Dr. Danielle Grogan, Research Scientist,

Earth Systems

On July 28th, 2021

Approval signatures are on file with the University of New Hampshire Graduate School.

ACKNOWLEDGEMENTS

I would like to thank my advisor, Dr. Bill McDowell, for his guidance and support throughout my pursuit of a master's degree. Thanks to my committee members, Dr. Kalle Matso and Dr. Danielle Grogan for their support throughout this project. I am grateful to my entire committee for being available, especially during our year of work-from-home. To Dr. Grogan, thank you for your help in project management with R and GitHub. Thanks to the Water Quality Analysis Lab and in particular Jody Potter, Aneliya Cox, and Allison Herreid, for general help with questions, lab training, field work, data QAQC, and R coding. Special thanks to Allison Herreid for editing. Thanks to Michelle Shattuck for providing data and for help with load calculations. Thank you to Dr. Adam Wymore for being an idea sounding board and Dr. Hannah Fazekas for help with R. To Chris Peter, thanks for being an incredible mentor at Great Bay. To those at the Piscataqua Estuaries Region Partnership, Great Bay National Estuarine Research Reserve, and Jackson Estuarine Laboratory, thank you for believing in this project and in me. I am looking forward to tackling the science and management of Great Bay in future collaborative projects. To my family and friends, thank you for your support, laughter, and understanding throughout these last two years. To Rick, thank you for your endless support and for being the first person to watch every practice presentation. Support for this research was provided by the NOAA Margaret A. Davidson Fellowship.

TABLE OF CONTENTS

LIST OF TABLES

LIST OF FIGURES

ABSTRACT

BIOGEOCHEMCIAL STRESSORS AND ECOLOGICAL RESPONSE IN GREAT BAY ESTUARY

By:

Anna Lowien

University of New Hampshire

Estuaries are threatened by eutrophication due to increasing anthropogenic nutrient loading from surrounding coastal watersheds. The Great Bay Estuary, NH/ME, has been designated as nitrogen impaired primarily due to a 44% loss in eelgrass coverage since 1996. Since 2014, wastewater treatment plants in the watershed have begun upgrading to reduce nitrogen loads to Great Bay. This region has also experienced changes in climate, with multiple, consecutive years of low annual precipitation totals. The loss of eelgrass, increased variability in precipitation, and continued anthropogenic land-use influence on the region have biogeochemical consequences for Great Bay. Solute budgets for a portion of Great Bay Estuary were developed at annual and monthly timescales for nitrogen, orthophosphate, dissolved organic carbon, and total suspended solids. Inputs and outputs of nutrients, carbon, and sediments have been monitored monthly since 2008, across both point and nonpoint sources. Results show total annual nitrogen input loads are less than output loads, indicating net export from Great Bay. Dissolved inorganic nitrogen annual inputs exceeded outputs on average, resulting in positive Δ storages values and indicating net import. Net ecosystem metabolism is an important driver of patterns in dissolved organic carbon, orthophosphate, and dissolved inorganic nitrogen retention. Black box models can aid resource managers with understanding the relative amounts of nutrients, carbon, and sediments an estuary is biogeochemically capable of retaining or exporting to the coastal ocean.

CHAPTER 1: INTRODUCTION

Estuaries function as key biogeochemical filters within the land-ocean continuum as they are conduits for the transfer of freshwater discharge to the coastal ocean. Globally, estuaries receive an estimated 27% of freshwater export to oceans, along with associated nutrients, carbon (C), and sediments (Laruelle et al., 2013). This hydrologic coupling of coastal watersheds to estuaries drives the exchange of nutrients, C, and sediments between fluvial freshwater and tidal marine ecosystems (Bauer et al., 2013; Bowen & Valiela, 2008; Feng et al., 2015; Regnier et al., 2013; Wild-Allen & Andrewartha, 2016). During this exchange, solute inputs can be retained within an estuary or exported to the coastal ocean (Cai & Wang, 1998; Wild-Allen & Andrewartha, 2016). The balance between net import (storage) and export, defines the biogeochemical role of estuaries (Bauer et al., 2013; Regnier et al., 2013; Wollast, 1983).

Estuaries become net exporters or importers of nutrients as a function of overall productivity. The 'outwelling' hypothesis states that estuaries become net exporters of nutrients when ecosystem productivity exceeds the level at which materials can be internally processed and stored (Flynn, 2008; Odum, 1980; Winter et al., 1996). This suggests two important driving mechanisms of an estuary's biogeochemical function. First, estuarine productivity directly affects the assimilation of nutrients and C production. Thus, estuaries influence the source or sink designation over seasonal and inter-annual timescales (Buzzelli et al., 2013; Flynn, 2008). Second, the ability of an estuary to process terrestrial inputs is limited by hydrodynamic flushing (Buzzelli et al., 2013). Large fluxes of materials into an estuary may not remain in the system long enough for biogeochemical transformation and instead rapidly flush out to the ocean. Together, ecosystem-level processes and human-and-climate-induced stressors determine

whether solutes move through an unreactive estuarine pipe to the coastal ocean or are actively produced (net export) and transformed (net import). Quantifying the biogeochemical role of estuaries presents a challenge due to inherent spatial and temporal variability of these driving processes.

Human and climate-induced stressors complicate estuarine biogeochemical cycles by creating imbalances in nutrient and C fluxes. An estimated 39% of the U.S. population lives in a coastal county and contributes additional sources of nutrients, C, and sediments to coastal ecosystems (Freeman et al., 2019). Anthropogenic nitrogen sources, ranging from wastewater treatment facilities and septic systems to fertilizer application, contribute higher nutrient loads to estuaries (Hopkinson & Vallino, 1995). Terrestrial inputs account for 34% of the global nitrogen flux between land and sea (Regnier et al., 2013; Seitzinger et al., 2005). This global flux is influenced by climate variability, with wetter years transporting more anthropogenic nitrogen than drier years (Howarth et al., 2006). The global phosphorus cycle has also been greatly impacted by anthropogenic activities, including fertilizer application and septic system leakages (Seitzinger et al., 2005). Globally, estuaries are estimated to receive around 0.7 Tg of terrestrial phosphorus each year (Regnier et al., 2013; Seitzinger et al., 2005). The ramifications of imbalanced nitrogen and phosphorus loads include the promotion of eutrophication events that subsequently can induce hypoxia and reduce light availability in an estuary (Diaz & Rosenberg, 2008; Ganju et al., 2014; Smyth et al., 2013).

Dissolved organic carbon (DOC) loads to estuaries are less directly impacted by anthropogenic activities, but rather originate primarily from terrestrial and estuarine primary production (Bauer

et al., 2013). Estuaries are usually net heterotrophic, indicating faster consumption of organic matter than *in situ* production or external terrestrial loading (Bauer et al., 2013). Global estimates suggest that rates of estuarine respiration exceed riverine load and estuarine production by 0.2 Pg C $year^{-1}$ and that estuaries release upwards of 0.25 Pg C $year^{-1}$ as CO_2 (Bauer et al., 2013). Total suspended solids (TSS) sources to an estuary can originate externally from a watershed or internally from sediment resuspension due to wave action, winds, or seagrass loss (Ganju et al., 2014; Lacy & Wyllie-Echeverria, 2011). Sediments are an important component of water quality in estuaries, because high concentrations can increase light attenuation and release dissolved forms of nitrogen and phosphorus back into the water column (Kirk, 1983; Percuoco et al., 2015).

The influence of human activities on coastal ecosystems has resulted in declines of many notable habitats, ranging from coral reefs to salt marshes. Nutrient imbalances within estuaries have contributed to high rates of seagrass meadow loss globally, with estimates suggesting between two and five percent of global seagrass coverage is lost annually (Duarte et al., 2008). Despite a high rate of decline and the highest ecosystem service valuation per hectare ($19,004 ha^{-1} $year^{-1}$), seagrass ecosystems receive substantially less attention from both researchers and the general public (Duarte et al., 2008). Seagrass decline is often an ecological indicator of eutrophication, as ephemeral macroalgae species respond to excess inputs of nitrogen and outcompete seagrasses for nutrients and light (Short et al., 1995; Valiela et al., 1997). In coastal systems with increasing nitrogen loads, macroalgae species have been shown to replace seagrass beds and contribute to a larger proportion of the total net ecosystem production (Valiela et al., 1997). Macroalgal species

have been shown to continue to expand in estuaries that surpass total nitrogen loading thresholds that detrimentally impact eelgrass coverage (Robertson & Savage, 2021).

This study focuses on Great Bay Estuary, where changing land use, growing population density, and climate change threaten the underlying hydrologic coupling that drives the loading of dissolved and particulate solutes to the estuary. Great Bay Estuary is currently designated as nitrogen impaired, in part due to the 17 wastewater treatment facilities that discharge into the estuary's tidal tributaries (Burdick et al., 2020). Wastewater treatment has been estimated to account for 50% of dissolved inorganic nitrogen (DIN) inputs to Great Bay Estuary (Piscataqua Region Estuaries Partnership, 2018). Additionally, Great Bay Estuary has lost 44% of its eelgrass coverage in two decades (Burdick et al., 2020). This loss has ramifications for biogeochemical cycles and ecosystem health, as eelgrass meadows provide a suite of ecosystem services, ranging from fish habitat (Chalifour et al., 2019), wave and current attenuation (Lacy & Wyllie-Echeverria, 2011), carbon sequestration in sediments (Oreska et al., 2017) and in biomass (Fourqurean et al., 2012) to nutrient cycling (Aoki et al., 2020).

It is critical to move beyond an understanding of watershed inputs to estuaries by studying the fate of ecologically important solutes. This is particularly crucial for Great Bay because the estuary faces N impairments, poor water clarity, and reduced eelgrass cover. Determining whether Great Bay functions as an unreactive pipe or active contributor to biogeochemical cycling will be vital to maintaining the balance between ecosystem health and human resource demand. Refining the role of estuaries in global biogeochemical cycles requires first an understanding of what is retained or lost through an estuarine filter and the factors influencing the proportion of each retention or loss pathway.

The purpose of this study was to assess the biogeochemical capacity of Great Bay Estuary to process inputs of nutrients, carbon, and sediments at varying temporal scales. I asked two questions: (1) How do patterns of input, retention, and output of nutrients, carbon, and sediments vary temporally? (2) How do above patterns in water quality influence biotic response, measured as eelgrass coverage, chlorophyll-a concentration, and net ecosystem metabolism in the estuary?

CHAPTER 2: METHODS

Study area

Great Bay Estuary is a shallow, well-mixed estuary located along the New Hampshire-Maine border (Bilgili et al., 2005). The drowned river valley is tidally connected to the Gulf of Maine via the Piscataqua River (Figure 1). Freshwater input originates from seven tidal tributaries in the 2,651 km^2 coastal watershed and on a decadal scale, constitutes 2% of the daily tidal prism ($178 \cdot 10^6$ m^3) (Short, 1992; Trowbridge, 2007). Water residence time averages between five and 20 days, depending on physical location within the estuary (Bilgili et al., 2005). Water depth varies with tide and topography, with eelgrass growing in the shallow subtidal and intertidal portions of the estuary. Average water depth across the estuary at mid-tide is 3.2 m (Trowbridge, 2007). This study was constrained to Great Bay, defined as the portion of the estuary south of the narrow outflow at Adams Point. Three of the seven tidal tributaries, the Lamprey, Squamscott, and Winnicut, flow directly into Great Bay. Mean annual (water year, n=11) discharge is the highest for the Lamprey (302 m^3 s^{-1}), followed by the Squamscott (108 m^3 s^{-1}), and then the Winnicut (27 m^3 s^-1). Additionally, three of the 17 municipal wastewater treatment facilities in the watershed discharge below the head-of-tide of tributaries to Great Bay.

Conceptual model: mass balance

To assess the magnitude of biogeochemical cycling in Great Bay, inputs and outputs of nutrients, dissolved organic carbon (DOC), and suspended solids (TSS) were compared across a 10-year period (2008 – 2018). This period of study was selected due to the availability of water quality monitoring data. A black box model approach was applied to calculate annual solute budgets with the equation:

$$\text{Inputs} - \text{Outputs} = \Delta \text{ Storage} \quad \{\text{Eq. 1}\}$$

Inputs and outputs of solutes were calculated as loads and the change in storage (Δ storage) values were normalized by Great Bay's surface area at mean high water level (1677 hectares). The black box approach assumes the study system is well-mixed, with steady-state hydrodynamic characteristics (Regnier et al., 2013).

The black box model was constrained to Great Bay. Solute inputs to Great Bay include four categories: point sources (wastewater treatment facilities), nonpoint sources (tributary, groundwater, and coastal runoff fluxes), direct atmospheric deposition (precipitation), and tidal flux (high tide) (Figure 2). It was assumed that high tide flux into Great Bay includes some wastewater treatment effluent from facilities that discharge into Little Bay and the Piscataqua River, but it was outside the scope of this study to estimate that amount. Solute output from Great Bay was defined as the outgoing ebb tide, past Adams Point and out to Little Bay and the Gulf of Maine. Monthly sampling events for solute concentrations were assumed to be representative of that month. The Δ storage term reflects any gain or loss within the system, including difficult-to-measure output pathways like denitrification and nitrogen fixation. This model includes any internal loss pathways (e.g., production and degassing of N_2 from denitrification) in the Δ storage term. Positive Δ storage values represent a net import into Great Bay and negative Δ storage values represent a net export from Great Bay.

Water quality data and load calculations

Water quality data were compiled from multiple sources, including long-term monitoring datasets, municipal reports, and published studies. Tidal tributaries were sampled monthly at the

head-of-tide between March and December each year as part of on-going water quality monitoring efforts (Matso & Potter, 2018). Estuarine water samples were collected monthly from Adams Point at high and low tide between January and December each year. Samples were filtered with pre-combusted Whatman GF/F filters and kept frozen in acid-washed polyethylene (HDPE) bottles until analyzed. Measurements of dissolved oxygen (percent saturation and concentration), water temperature (°C), and specific conductance (μS cm^{-1}) were recorded at the time of sample collection with a YSI multiparameter probe (YSI ProDSS). For more details regarding the riverine and estuarine datasets, please see the Great Bay Estuary Tidal Tributary Monitoring Program: Quality Assurance Project Plan (https://scholars.unh.edu/prep/406) and the Great Bay Estuary Water Quality Monitoring Program: Quality Assurance Project Plan (https://scholars.unh.edu/prep/405/).

Atmospheric wet deposition over Great Bay was estimated using weekly precipitation collector data from Thompson Farm in Durham, NH. In October of 2008, the collection system was switched from an Aerochem Metrics 301 precipitation collector to a N-Con Systems Atmospheric Deposition Sampler, placed at the top of a flux tower (Liptzin et al., 2013). The combined dataset from the two collectors at Thompson Farm was used for calculation of precipitation (wet deposition) solute loads. Hourly precipitation totals (mm) were downloaded from the NCDC U.S. Climate Reference Network. Precipitation totals were summed by the weekly monitoring period and calendar year.

Tributary, estuarine, and precipitation water samples were analyzed for a suite of dissolved and particulate constituents. Samples were analyzed for total dissolved nitrogen (TDN) and dissolved

organic carbon (DOC) using high-temperature catalytic oxidation, for ammonium (NH_4^+) with automated colorimetry (SmartChem 200 discrete analyzer), and for phosphate (PO_4^{3-}) and nitrate plus nitrite (NO_3^-+NO_2^-) using automated colorimetry (Seal AQ2). An unfiltered sample was analyzed for total nitrogen (TN) with alkaline persulfate digestion and automated colorimetry (Seal AQ2). Total suspended solids (TSS) was calculated as the mass per unit volume of suspended solids retained and dried on a 0.7 μm filter. TSS filters are subsequently combusted and analyzed for particulate nitrogen (PN) (Perkin Elmer 2400 Series 11 CHN Elemental Analyzer). Dissolved Organic Nitrogen (DON) was calculated as the difference between TDN and DIN (NH_4^+ + NO_3^- + NO_2^-). From 2015 onward, TN was calculated as the summation of PN and TDN.

Solute concentrations below an instrument's method detection limit were set to one-half of the detection limit. As DON is a calculated variable, method detection limit was determined to be 5% of the sum of TDN, NO_3^- + NO_2^-, and NH_4^+ concentrations. Calculated DON wet deposition concentrations are often negative, due to the low amount of organic nitrogen found in wet deposition (Hill et al., 2005; Neff et al., 2002). Consequently, concentrations of wet deposition DON were set to half the method detection limit if the absolute value of the DON concentration was less than that of the calculated method detection limit. Any remaining negative DON concentrations were left in the dataset, as removing those values would bias the data set and result in an overestimation of DON precipitation loads.

Tributary annual loads for solutes were calculated as the product of the annual flow-weighted concentration and annual discharge. Loads were calculated for years with a minimum of eight

collected water samples. Mean daily discharge was downloaded for the period of interest from a USGS gauge on each river (https://waterdata.usgs.gov). As the locations of the USGS stream gauges and the head-of-tide water quality sampling stations differed, a flow multiplier was used to estimate discharge at the head-of-tide (Appendix A, Table A1). The flow multiplier was calculated as the ratio of watershed area at the head-of-tide and the watershed area at the stream gauge. Flow-weighted annual concentrations were calculated using the following equation, where *C* is the concentration of a solute on a given sampling day, *i*, and *Q* is the mean daily discharge, corrected by the flow multiplier:

$$\frac{\sum C_i Q_i}{\sum Q_i} \quad \{\text{Eq. 2}\}$$

High and low tide loads at Adams Point were calculated using concentration data at high and low tide and the tidal prism. The tidal prism is the total volume of oceanic water that moves into and out of Great Bay in a set time. The reported average daily tidal prism for Great Bay Estuary is 178×10^6 m^3 (Trowbridge, 2007). The tidal prism was scaled to Great Bay using a ratio of surface area. To improve the tidal prism estimate for Great Bay, the volume of freshwater input to Great Bay, which was calculated as the summation of the tidal tributary mean daily discharges, corrected with flow multipliers, was subtracted out. Solute loads at Adams Point were then calculated as the product of the annual average concentration and the adjusted tidal prism, scaled to an annual rate.

Precipitation loads were calculated as the product of precipitation-weighted annual concentration, annual precipitation total (mm), and Great Bay's surface area. The precipitation-weighted annual concentration was calculated using the following equation, where *C* is the

concentration of a solute on a given sampling day, *i*, and *P* is the precipitation total for the period the collector bucket was left out to collect wet deposition:

$$\frac{\sum C_i P_i}{\sum P_i} \quad \{\text{Eq. 3}\}$$

Normalized loads were multiplied by the surface area of Great Bay at mean high tide to get total direct loads in kg year^{-1}.

Monthly loads for riverine, estuarine, and precipitation were calculated in a similar manner to annual loads, but with a monthly flow or precipitation-weighted concentration instead of an annual concentration. For precipitation monthly loads, a weighted concentration was only used if there were more than two sampling dates in each month with sufficient volumes for solute analyses.

Water quality data from wastewater treatment facilities varied by facility. Where available, monthly TN and TSS loads were calculated as the product of monthly average concentration and average effluent flow. Monthly loads were summed for annual loading estimates. Loads from the Newfields wastewater treatment facility were calculated with monthly reported effluent flows and an annual average TN and DIN concentration from Bolster 2002. Newfields is a small wastewater treatment facility, with an average effluent discharge of 5.4% ± 1.1 that of Exeter's rate of effluent discharge. Due to this small footprint, it was deemed acceptable to use the 2002 nitrogen concentrations with the updated monthly flow rates to calculate loads. In instances where DIN concentrations were unknown, DIN load was assumed to be 84% of the annual TN load. This assumption is based on the average DIN:TN ratio of other wastewater treatment facilities in the Great Bay Estuary watershed (Piscataqua Region Estuaries Partnership, 2017). A

high DIN:TN ratio is reasonable as all three wastewater treatment facilities had primary and secondary treatment systems – meaning that most solids containing particulate nitrogen would be removed before the effluent is discharged to Great Bay. As no data on DON were available, it was assumed that DIN concentrations equaled TDN concentrations. Concentrations of DOC and PO_4^{3-} for the wastewater treatment facilities were not available at the same measurement frequency as TN. A DOC:TDN ratio across three wastewater treatment facilities was calculated from limited monitoring data for Epping, Exeter, and Newfields. The ratio was then applied to annual DIN loads to estimate DOC loads. An N:P ratio calculated from monitoring of the Epping wastewater treatment facility was applied to annual DIN loads to estimate PO_4^{3-} loads. Ratios were calculated using solute concentrations.

A published direct groundwater dissolved inorganic nitrogen (DIN) load of 6,800 ± 7,500 kg N year $^{-1}$ for Great Bay was used for groundwater inputs (Ballestero et al., 2004). As no other groundwater loading values were available, it was assumed this rate of groundwater loading was consistent year-to-year. It was assumed that TN groundwater loading was similar to the reported DIN loads, due to filtration of particulate nitrogen as water flows through the unsaturated zone (DeSimone & Howes, 1998). No studies on direct groundwater contributions to Great Bay have quantified loads for orthophosphate, DOC, or DON. This model assumed that groundwater inputs of those variables were negligible. Direct coastal runoff loads from land adjacent to Great Bay were estimated by multiplying the Lamprey River watershed yields for each solute (area normalized load) by the drainage area surrounding Great Bay that lacks monitored tributaries (~37 km^2).

Comparison of input and output concentrations

An alternative black box model approach focused on the difference in average input concentration and average output concentration at the Adams Point outlet. This model version assumed that solute concentrations at high and low tide were the same for Great Bay. This assumption was tested by first assessing the normality of tidal solute concentrations at Adams Point. Raw concentrations failed the Shapiro-Wilk normality test. Rather than transform the dataset, which would interfere with direct interpretation of the concentration comparison results, a nonparametric, Wilcoxon Mann-Whiney U-test, was used to compare high and low tide concentrations. Concentration-based comparisons were considered for solutes only if the high and low tide concentrations were deemed not statistically different by the Wilcoxon Mann-Whiney U-test. The mean annual average solute concentrations of tributary (volume-weighted), wastewater treatment, and precipitation (volume-weighted) inputs were compared to the annual average estuarine concentration at Adams Point. If concentration of these inputs differed from the average estuarine concentration at Adams Point, it would indicate the removal or addition of that solute within Great Bay.

The influence of river solute concentrations on observed estuarine concentrations at Adams Point, was determined through dilution calculations at a decadal time-step. Decadal average flow-weighted concentrations and decadal average discharge for the Lamprey, Squamscott, and Winnicut, along with the average tidal prism volume for Great Bay, were used to calculate the expected concentration of river nitrogen in Great Bay. This calculation assumed the rivers were the only input of TN and DIN.

Ecological data

Ecological data were obtained from multiple monitoring efforts. Chlorophyll-a, a proxy for algal presence, was measured monthly at the tributary head-of-tide and estuarine monitoring sites. A 1L sample of unfiltered water was collected in an acid washed HPDE bottle, kept on ice until returned to the laboratory, and then filtered on a pre-combusted 0.7 μm Whatman GF/F filter. Chlorophyll-a concentrations were corrected for phaeophytin concentrations. Eelgrass coverage (total area that contains a minimum of 10% cover) has been estimated in Great Bay at an annual timestep using aerial photography (Barker, 2018, 2020; Short, 2016) (Appendix B, Figure B1).

Net ecosystem metabolism was calculated using the SWMPr and WtRegDO packages in R (version 4.0.3), according to the oxygen-based open water method (Odum, 1956) and described in Beck et al. (2015). This method calculates total primary production and total ecosystem respiration using diel changes in oxygen. Continuous (15-minute record) dissolved oxygen, depth, and tide data were downloaded from the National Estuarine Research Reserve Central Data Management Office (https://cdmo.baruch.sc.edu/) for the central monitoring station in Great Bay. YSI EXO2 data sondes were deployed throughout the estuary between April and December each year, as part of the National Estuarine Research Reserve System Wide Monitoring Program. The dissolved oxygen record was de-tided to remove the influence of wave action on dissolved oxygen concentrations and to isolate the biological, diel signal. Due to differences in depth records, net ecosystem metabolism was only calculated from 2014, onward, at both an annual and monthly time step.

Statistical analyses

Standard error for the multi-annual average of each solute's inputs and outputs was calculated, following methods outlined by Lehrter & Cebrian (2010). If inputs were estimated from the literature or from known values of other inputs, standard errors could not be calculated. Uncertainty for the box model Δ storage values was assessed by first determining the range in inputs and outputs for each solute. The possibility of Δ storage values flipping in sign was tested by comparing the end-member range of solute inputs and outputs. This was accomplished two different ways: 1) by looking at range in possible loads based on calculated standard deviations for inputs and outputs and 2) comparing the highest input year load to the lowest output year load and vice versa. For the first, above-mentioned, method, the range in loads was either based on the standard deviation range for concentrations or loads (if concentration data was not used in the box model – i.e., groundwater estimate). The standard deviation is calculated from the range of the 11 annual input and output values – i.e., it represents interannual variability, and not measurement uncertainty. All data was assessed for skewness, kurtosis, and covariance prior to analysis. In all instances, skewness was < 2. Kurtosis varied with each solute and mass balance component. In general, kurtosis was higher in the calculated Δ storage values than in the inputs or outputs. One-way analysis of variance (ANOVA) was used to detect differences in monthly solute loads across months. Tukey's honest significance test for multiple comparisons was used as a post hoc test to determine which months differed in mean solute load for TN, PN, DIN, DOC, PO_4^{3-}, and TSS. Bivariate relationships between solute concentrations, solute loads, physiochemical parameters, and ecological response variables were assessed using correlation and simple linear regression analysis. All calculations and statistics can be found in a publicly available GitHub Repository (https://github.com/ALowien/GreatBay_BoxModel).

CHAPTER 3: RESULTS

Solute concentrations across inputs and outputs

Results of Wilcoxon Mann-Whiney U tests showed no significant differences between Adams Point high and low tide concentrations of dissolved inorganic nitrogen (DIN), orthophosphate (PO_4^{3-}), and dissolved organic carbon (DOC) (Table 1). Wilcoxon Mann-Whiney U-test results for total nitrogen (TN) and particulate nitrogen (PN) showed significant differences between high and low tide concentrations ($p < 0.05$). Average TN concentration at low tide was 11% greater than average total nitrogen concentration at high tide. Similarly, PN average concentration was 25% greater at low tide, compared to high tide concentrations. Despite having statistically different means, the standard deviations for TN concentrations at high and low tide indicate substantial overlap between the two distributions. The high tide average concentration of TN becomes greater than the low tide concentration, when the higher and lower ends of the standard deviations are applied, respectively, to the high and low tide concentrations.

Average flow-weighted tributary and average wastewater treatment concentrations of TN exceeded the estuarine concentration at Adams Point (Table 2). At a decadal time step, the high river TN concentrations do not exert a large influence on the estuary, as river TN concentrations are expected to dilute down to 0.009 mg N L^{-1} within the estuary, if mixed with pure seawater containing no TN. This expected dilution is less than the method detection limit for TN (0.02 mg-N L^{-1}), but does not include wastewater inputs below the tributary head-of-tide monitoring stations. Average DIN tributary concentrations ranged between 0.13 and 0.19 mg N L^{-1} (Table 2) and were similar to the average estuarine outflow concentration. The decadal average of riverine concentrations of DIN to Great Bay would dilute down, on average, to 0.003 mg N L^{-1} over

background concentrations in high tide samples. Tributary DOC inputs to Great Bay exceeded the estuarine concentration, on average, by 4.34 mg C L^{-1}, indicating higher input of DOC than output. Orthophosphate concentrations were the most similar across freshwater inputs and estuarine concentrations, exhibiting a nearly net balance between concentration inputs and outputs.

At a daily time-step, freshwater input influenced estuarine concentrations. Freshwater input from Great Bay's tidal tributaries explained between 4% and 22% of the variability in solute concentrations at low tide (Figure 3). DIN, DOC, PN, and TN concentrations all increased with increasing freshwater input and had significant positive slopes ($p < 0.05$). PO_4^{3-} concentrations behaved inversely, decreasing with increasing freshwater input ($R^2 = 0.18$, $p < 0.05$). Freshwater input explained the most variability in DOC concentrations at low tide, with an R^2 of 0.22.

Inter-annual variability in solute budgets

Inputs of TN, normalized by surface area of Great Bay at mean high tide, ranged from 3,200 to 5,100 kg N ha^{-1} $year^{-1}$. TN output, on average, exceeded inputs by 7% across the decade. Output yields ranged from 3,200 to 5,600 kg N ha^{-1} (Figure 4A). Inputs of PN, normalized by Great Bay mean high tide surface area, ranged from 630 to 1,080 kg N ha^{-1} $year^{-1}$. PN outputs ranged from 750 to 1,600 kg N ha^{-1} $year^{-1}$ (Figure 4C). PN annual loads represented 22% (± 3.7%) of total nitrogen input to Great Bay and 27% (± 6.2%) of total nitrogen output from Great Bay. While PN inputs could have been underestimated between 2008 and 2012 due to only having high and low tide PN concentration data, it is unlikely to be significant. Tributary PN loads between 2013 and 2018 contributed only 1-2% of the high tide PN input load each year, based on monthly grab

samples of tributary PN. TN (Figure 4B) and PN (Figure 4D) had average Δ storage yields of -277 and -284 kg N ha^{-1} $year^{-1}$, respectively, across the 10-year study period. In 2017, both TN and PN Δ storage were positive, due to loading inputs exceeding output that year. The increase in TN and PN input loads in 2017 was likely driven by the increase in freshwater inputs that year. Annual freshwater input increased 63% between 2016 and 2017 (Appendix B, Figure B3).

Annual DIN Δ storage values trended in the opposite direction of the TN and PN yields, with an average Δ storage value of 146 kg N ha^{-1} $year^{-1}$ (n=8). DIN inputs ranged from 1,100 to 2100 kg N ha^{-1} $year^{-1}$ and outputs ranged from 900 to 1700 kg N ha^{-1} $year^{-1}$ (Figure 5). Annual inputs of DIN, on average (n=9), represented 37% (± 5.3%) of TN loads into to Great Bay and 31% (± 5.6%) of TN output. Average DOC input and output yields nearly balanced each year, with an average input of 32,600 kg C ha^{-1} $year^{-1}$ (n =8) and average output of 32,700 kg C ha^{-1} $year^{-1}$ (Figure 6). Between 2015 and 2018, both DOC inputs and outputs increased, with inputs outpacing outputs in 2017. DOC inputs to Great Bay increased 68% between 2015 and 2018 and DOC outputs increased 52% over the same period. This increase is attributable to increases in both high and low tide concentrations, and therefore loads. High tide DOC load into Great Bay increased at an average rate of 8.9×10^{6} kg C $year^{-1}$ over the 4-year period.

Orthophosphate yields into and out of Great Bay resulted in a net positive Δ storage (19 kg ha^{-1} $year^{-1}$). Inputs of orthophosphate ranged from 190 to 300 kg P ha^{-1} $year^{-1}$ and output from Great Bay ranged from 170 to 272 kg ha^{-1} $year^{-1}$ (Figure 7). The average ratio of DIN:PO_4^{3-} (mass ratio of input loads) across year was 6.2 ± 1.8. The DIN:PO_4^{3-} ratio of outputs was slightly lower, at

5.9 ± 1.8. Output of TSS exceeded input every year, resulting in an average Δ storage of -276 kg ha^{-1} $year^{-1}$ (Figure 8).

Uncertainty in inter-annual solute budgets

Due to underlying assumptions in a mass balance solute budget, there is some uncertainty in determining input and output for a given year. Standard error for tidal input and output of TN was 4% of the mean. Wastewater treatment facility inputs of TN had standard errors that ranged from 1 to 12% of the mean load. Tributary inputs had the highest standard errors for TN, ranging from 10% of the mean for the Lamprey to 13% of the Squamscott mean annual load. DIN standard errors across inputs and outputs mirrored those of TN. Across inputs and outputs, standard error for phosphate ranged from 1-17% of the mean, with the Lamprey River annual loads having the highest standard error. DOC standard errors ranged from 1 to 18% of a given input or output multi-annual mean. Precipitation DOC input had the highest standard error relative to the mean. TSS standard errors ranged from 6% to 42% of the mean TSS load.

Comparison of the highest annual TN input load and lowest annual output load (and vice versa) suggested that Δ storage estimates could vary between -4.0×10^6 and 3.2×10^6 kg N $year^{-1}$. Based on the standard deviation of various input concentrations and loads, the measurement uncertainty for the TN Δ storage term ranges between -4.4×10^6 and 3.5×10^6 kg N $year^{-1}$ (Appendix A, Table A4). This wide range in uncertainty encompasses all the individual annual storage estimates for TN. The range in uncertainty for TN Δ storage term is more heavily weighted towards the negative end of the range.

Estimates of Δ storage for DIN, based on comparing the highest inputs and lowest outputs and lowest inputs and highest outputs, ranged from -9.3×10^5 to 1.9×10^6 kg N year^{-1}. This was a narrower range than that calculated based on the range in standard deviations (Appendix A, Table A4). The uncertainty range for DIN Δ storage terms had a wider positive range than negative range. Based on the standard deviation range for DOC, the uncertainty in the Δ storage term ranged from -3.2×10^7 to 3.4×10^7 kg C year^{-1} (Appendix A, Table A4). Comparison of the highest input to lowest output loads and lowest input to highest output loads resulted in a similar uncertainty range (-3.2×10^7 to 2.3×10^7 kg C year^{-1}). Uncertainty for the orthophosphate Δ term ranged from -4.2×10^5 to 4.9×10^5kg P year^{-1} (Appendix A, Table A4). The range in uncertainty for DOC and orthophosphate showed the most balance, with the relatively same low (negative) and high (positive) endmembers.

Intra-annual variability in solute budgets

Mean DIN monthly input and output yields exhibited seasonal variation, with minimum yields in July and maximum yields in December (Figure 9A and 9B). Analysis of variance showed significant differences in mean DIN monthly inputs ($p < 0.05$) and mean DIN monthly outputs ($p < 0.05$). Monthly input yields ranged from a mean of 63 kg N ha^{-1} month^{-1} to 180 kg N ha^{-1} month^{-1}. Monthly output yields ranged from a mean of 52 kg N ha^{-1} month^{-1} to 182 kg N ha^{-1} month^{-1}. Post hoc comparisons using the Tukey HSD test revealed that December inputs were significantly greater ($p < 0.05$) than spring and summer inputs. DIN output in December was significantly different than summer and early fall outputs ($p < 0.05$). DIN monthly outputs mostly exceeded inputs, except in May, November, and December, resulting in most months averaging a positive Δ storage for DIN (Figure 9C). The monthly mean DIN Δ storage ranged

from -5 kg N ha^{-1} $month^{-1}$ in May to 40 kg N ha^{-1} $month^{-1}$ in September. Analysis of variance showed no significant difference in DIN Δ storage across months ($p > 0.05$).

Dissolved organic carbon monthly input, output, and Δ storage yields did not significantly differ between months. Inputs ranged from 2,200 kg C ha^{-1} $month^{-1}$ in October to 3,200 kg C ha^{-1} $month^{-1}$ in April (Figure 10A). Output yield of DOC had a smaller range, with a minimum monthly average of 2,300 kg C ha^{-1} $month^{-1}$ and maximum of 3,100 kg C ha^{-1} $month^{-1}$ (Figure 10C). Storage of DOC within Great Bay varied each month, often alternating between positive and negative mean values. Average storage yields of DOC towards the end of the growing season (Fall) were tightly constrained, ranging from -106 kg C ha^{-1} $month^{-1}$ in November to -49 kg C ha^{-1} $month^{-1}$ in September (Figure 10C).

Analysis of variance of orthophosphate monthly input and output yields showed a significant difference between months ($p < 0.05$). Monthly mean inputs of PO_4^{3-} ranged from 7 kg P ha^{-1} $month^{-1}$ in March to 34 kg P ha^{-1} $month^{-1}$ in September (Figure 11A). Monthly mean outputs followed a similar pattern, with the monthly minimum occurring in April and the maximum in September (Figure 11B). Post hoc comparison (Tukey HSD) of monthly inputs demonstrated a significance difference between late summer and spring. Post hoc comparison using the Tukey HSD test also showed a significant difference between fall and winter PO_4^{3-} outputs and spring outputs ($p < 0.05$). Despite seasonal differences in inputs and outputs in PO_4^{3-} yields, Δ values did not have any significant differences across months. July had the lowest mean storage of -2 kg kg P ha^{-1} $month^{-1}$ and December had the highest, 6 kg P ha^{-1} $month^{-1}$ (Figure 11C). Monthly median molar ratios of DIN:PO_4^{3-} switched between phosphorus limitation in the spring (>16:1)

and nitrogen limitation in the summer and fall (< 16:1) (Figure 12). Ratios of DIN:PO_4^{3-} showed a wide seasonal range, with median input ratios ranging from 6.1 to 36.1 and output ratios ranging from 3.15 to 40.4.

Ecological Response

Since 1996, eelgrass coverage in Great Bay has declined by 42% (Appendix B, Figure B1), with 2019 surveys reporting 600 hectares compared to 1000 hectares in 1996. Annual precipitation totals in the region also showed a significant decreasing trend over time (Appendix B Figure B2). There was no significant correlation between annual eelgrass coverage and annual precipitation totals ($p > 0.05$). None of the loading terms (inputs, outputs, Δ storage) explained a significant amount of the variability in annual eelgrass coverage.

Annual average chlorophyll-a concentrations at Adams Point during high tide ranged from 1.92 μg L^{-1} in 2009 to 7.04 μg L^{-1} in 2014 (Figure 13). At low tide, annual chlorophyll-a concentrations ranged between 2.56 and 8.78 μg L^{-1}. Chlorophyll-a concentrations at Adams point did not exhibit an annual trend, but annual average concentrations were higher at low tide every year. Average chlorophyll-a concentrations at high and low tide did not show significant relationships with any of the ecosystem metabolism variables or solute loads.

Great Bay fluctuated between net heterotrophic and net autotrophic between 2014 and 2018. Mean annual net ecosystem metabolism ranged from – 2.6 mmol O_2 m^{-2} d^{-1} in 2017 to a maximum of 3.7 mmol O_2 m^{-2} d^{-1} in 2015 (Table 3). DIN input loads explained 82% of the variability in net ecosystem metabolism ($p < 0.05$) (Figure 14). Net ecosystem metabolism

shifted towards net heterotrophic in years with higher DIN input loads. Mean annual ecosystem respiration showed a strong, negative correlation with DOC input loads ($r = -0.97$). Annual DOC loads to Great Bay explained 92% of the variability in estimates of mean annual respiration rate ($p < 0.05$) (Figure 15A). Mean annual primary production rates explained 99% of the variability in annual DOC output loads from Great Bay (Figure 15B). At a monthly time-step, both primary production and ecosystem respiration peaked in the summer months (Figure 16). Between 2016 and 2019, the magnitude of primary production and respiration increased each year. For example, the July primary productivity rate increased by 39% between 2017 and 2018 and by 36% between 2018 and 2019.

CHAPTER 4: DISCUSSION

Great Bay exports particulate nitrogen and retains dissolved inorganic nitrogen

Net export (– Δ storage values) of particulate nitrogen (PN) and total nitrogen (TN) from Great Bay is likely driven by internal sources, including resuspension of the sediment bed and export of nitrogen-rich detritus. These internal contributions to the PN and TN pools tip the balance between inputs and outputs, resulting in more nitrogen leaving Great Bay than entering. The net export of PN and TN to the coastal ocean has been documented in other estuaries globally, including temperate and tropical systems (Baird et al., 1987; Boynton et al., 1995; Nixon et al., 1996; Young et al., 2005; Zuo et al., 2016). The Chesapeake Bay system, another eutrophic estuary, is estimated to export 45.88×10^6 kg N $year^{-1}$ seaward, as total nitrogen (Boynton et al., 1995). The average output flux of TN from Great Bay is of the same order of magnitude, at 71.55×10^6 kg N $year^{-1}$. In the East China Sea, PN export was 1.37 times the input flux (Zuo et al., 2016). For comparison, the ratio of average output to input flux was 1.1 for TN and 1.3 for PN in Great Bay.

Rates of resuspension of particulate nitrogen into the water column and subsequent export from estuaries is a function of residence time, presence/absence of submerged aquatic vegetation, and sediment grain size (Baird et al., 1987; Nixon et al., 1996). Nixon et al. (1996) examined annual nitrogen budgets for nine estuaries that varied in size and nutrient loading rate and found that total nitrogen export from estuaries decreases with increasing water residence time in the system. This suggests that lower residence times promotes flushing of particulates from a system faster than they can be retained. Baird et al. (1987) found that particulate organic nitrogen concentrations were typically higher during ebb tides than during flood tides, with the highest

concentrations occurring closer to the end of the ebb, or outgoing, tide. In Japan, particulate organic matter fluxes in macrotidal estuaries showed similar results with particulate organic nitrogen concentrations increasing towards low tide (Takasu et al., 2020). It is suggested that strong tidal currents associated with the outgoing tide create active resuspension of sediments (Takasu et al., 2020). This pattern of higher PN and TN concentrations near low tide is consistent with findings for Great Bay, where low tide concentrations of both solutes were significantly different from and higher than high tide concentrations.

Eelgrass coverage decline in Great Bay has likely contributed to higher bed shear stress and consequently higher rates of sediment resuspension that contribute to particulate nutrient fluxes. The ecosystem service of sediment trapping by submerged aquatic vegetation is well documented within estuaries (Barbier et al., 2011; de Boer, 2007; Hansen & Reidenbach, 2013; Zhang et al., 2020). *Zostera marina* meadows have been shown to reduce tidal wave heights by 25% to 49% and to reduce wave energy by 34% (Fonseca & Cahalan, 1992; Reidenbach & Thomas, 2018). The high sediment mud fraction in Great Bay (>25%) means that bare sediments are even more vulnerable to resuspension events, as smaller particles have lower critical shear stress thresholds (Cook, 2019; Wengrove et al., 2015). PN concentrations tend to be higher in more turbid estuaries (Sarma et al., 2014), which is consistent with the observation that mean annual total suspended solids (TSS) output is 27% higher than mean annual TSS inputs in Great Bay.

Eelgrass, macroalgae, and phytoplankton in Great Bay also contribute to PN export, through production of living tissues and their subsequent decomposition. Estuaries are highly productive

ecosystems that support the growth of eelgrass, macroalgae, and phytoplankton. This primary productivity could, in turn, support the generation of particulate nitrogen. Leaf-bound nitrogen is the most likely form of organic nitrogen to be lost from *Zostera marina*, accounting for 78% of nitrogen loss from live plants (Risgaard-Petersen et al., 1998). Loss of fresh and senescent eelgrass leaves can range anywhere from 1 to 30% of eelgrass primary productivity (Bach et al., 1986; Hemminga et al., 1991). Movement of phytoplankton with the tides may also contribute to the particulate nitrogen export, as the decadal low tide average chlorophyll-a concentration at Adams Point was 27% higher than the high tide concentration. Chlorophyll-a concentrations are not always a perfect proxy for phytoplankton, as water grab samples at a monthly time-step may not always be representative of actual conditions. The concentration of chlorophyll in phytoplankton can vary with species and environmental conditions, such as temperature and water residence times (Alvarez-Fernandez & Riegman, 2014; Odebrecht et al., 2015).

Macroalgae cover and abundance was not included in this study due to a lack of spatially and temporally robust data. While macroalgae monitoring has occurred at a variety of sites throughout Great Bay, it represents a small subsample of the entire estuary and a limited time period (two – five years for a given site) (Burdick et al., 2019). The assessment of macroalgae cover at the quadrat scale is difficult to scale to an estuary wide estimate, making direct comparisons to bay-wide box model results also hard. Many of the macroalgae species of interest are detached, meaning they do not root within an ecosystem. This detachment means macroalgae is subject to tidal currents and winds, which influence the drift and accumulation of algal mats (Bell & Hall, 1997).

The stark contrast between net PN export and net DIN retention in Great Bay is indicative of transformation and transfer of nitrogen between the dissolved and particulate pools. Retention of DIN is likely driven by a combination of temperature-dependent biogeochemical pathways (i.e., biotic assimilation and denitrification). As DIN is retained (+ Δ storage), it is likely taken up by primary producers and eventually recycled into particulate organic nitrogen. The James River Estuary shows a similar mass balance result to the 10% DIN retention seen in Great Bay, retaining 37% of ammonium inputs and 18% of nitrate inputs (Bukaveckas et al., 2018). DIN retention within the James River Estuary was strongly influenced by water temperature, with peaks in retention occurring in the summer when temperatures were warmer, and discharge was lower (Bukaveckas et al., 2018). While there was not a significant difference in DIN monthly Δ storage values, September and August had the highest mean monthly DIN Δ storage values. This corresponds to the seasonal high for water temperature, with August and September averaging 22°C and 19°C, respectively. Bukaveckas et al. (2018) found that DIN retention was 10x higher when water temperatures exceeded 20°C versus when water temperatures were less than 15°C, indicating that temperature dependent biological processes, like biotic assimilation and denitrification, increased retention capacity within the estuary.

Total nitrogen uptake by *Zostera marina* varies, with estimates as low as 2.62 g N m^{-2} $year^{-1}$ (Aoki et al., 2020) and as high as 34.5 g N m^{-2} $year^{-1}$ in Denmark (Pedersen & Borum, 1993). Applying those uptake rates to annual Great Bay eelgrass coverage estimates and scaling by surface area at mean high tide, results in average (n = 9) eelgrass uptake of 9.52 kg N ha^{-1} $year^{-1}$ and 125.3 kg N ha^{-1} $year^{-1}$, respectively. That is between 6.3% and 86% of the average estimate of DIN Δ storage and between 3.4% to 45% of the annual average estimate of TN Δ storage.

Since TN storage values were mostly negative, it is more likely that eelgrass is taking up dissolved forms of nitrogen from the water column or sediment bed. Nitrogen assimilated by eelgrass and more ephemeral macroalgal species (i.e., *Gracilaria* species) represents a short-term storage or retention pathway. It is likely that much of the nitrogen bound to *Zostera marina* is slowly returned to the dissolved inorganic and particulate nitrogen pools during decomposition processes. Nitrogen retained in detritus can be mineralized and recycled within the ecosystem (Aoki et al., 2020). Decomposition processes are often slow within estuarine sediment beds, potentially creating a time-lag between N assimilation in live tissues and mineralization of detritus-bound N (Bach et al., 1986).

Continued high DIN retention within Great Bay, despite reductions in eelgrass coverage over time, suggests that other species (e.g., macroalgae and phytoplankton) are taking up nitrogen. Increasing algal cover within Great Bay has corresponded with decreases in eelgrass cover over time (Burdick et al., 2017). As of 2016, high levels of cover for red, green, and brown algae were found across eight different, intertidal, monitoring sites (Burdick et al., 2017). In particular, intertidal sites closest to subtidal eelgrass habitats were found to have the highest amount of cover of red and green algal species (Burdick et al., 2017). As monitoring has continued, intertidal sites within Great Bay saw decreasing percent cover of both green and red algae, but increasing brown algae cover between 2013 and 2018 (Burdick et al., 2019). The increase in brown algae while eelgrass continues to decline in Great Bay may explain why DIN storage values remain at the relatively same magnitude over the 10-year study period and why primary productivity continues to increase each year. The most recent declines in algal cover in Great Bay may be an indication of the system beginning to respond to point source reductions in

nitrogen loading, which could in turn influence box model results for nitrogen storage in the future.

Denitrification rates in estuaries vary by habitat type, with highest rates typically observed in fully vegetated eelgrass meadows (Aoki & McGlathery, 2017; Eyre et al., 2016) and lowest in subtidal and intertidal mud flats (Eyre et al., 2016). Aoki et al. (2020) report an annual denitrification rate of 0.62 g N m^{-2} $year^{-1}$ in eelgrass meadows and a bare sediment rate that is one-quarter of that (0.16 g N m^{-2} $year^{-1}$). Scaling the eelgrass meadow denitrification rate by annual eelgrass coverage in Great Bay and normalizing by estuary surface area, results in a mean denitrification rate of 2.25 ± 0.25 kg N ha^{-1} $year^{-1}$ (n=9). This suggests, without any *in-situ* measurements, that denitrification within Great Bay contributes very little to overall N storage/transformation (about 1.5% of estimated mean annual DIN storage). One major difference between Great Bay and the South Bay estuary studied by Aoki et al. (2020) is the degree of eutrophication, with Great Bay receiving more than 10x the N load per hectare than South Bay. Eutrophic estuaries have higher nitrate availability, which typically fuels greater rates of denitrification (Seitzinger et al., 2006; Welsh et al., 2001). Consequently, the contribution of denitrification to nitrogen removal in the eutrophic Great Bay system is likely underestimated.

Potential sources of nitrogen to fuel net export

The net nitrogen export from Great Bay is likely the result of multiple internal processes, including nitrogen fixation, erosion of the sediment bed, and primary production of living tissues. The last two of these processes have been discussed above, leaving the possibility of nitrogen fixation as an additional nitrogen source. The coupling of nitrogen fixation and

denitrification in eelgrass beds has been documented by many (Aoki et al., 2020; Capone, 1982; Cole & McGlathery, 2012; Iizumi et al., 1980; McGlathery et al., 1998). Eelgrass beds drive nitrogen cycling processes through direct assimilation of dissolved inorganic nitrogen species and through alteration of their immediate environment through labile carbon and oxygen production in the rhizosphere (Iizumi et al., 1980; Penhale & Smith, 1977; Thursby & Harlin, 1982). Cole & McGlathery (2012) show that nitrogen fixation in *Zostera marina* beds contributes 28x more nitrogen than fixation in bare sediments. The balance between fixation and denitrification is driven by the spatial variability in redox conditions within the sediment bed, as oxygenated zones are located close to root systems of submerged aquatic species (McGlathery et al., 1998). Although nitrogen fixation is likely occurring in remaining eelgrass beds within Great Bay, fixation alone cannot explain the net total and particulate nitrogen export. Nitrogen fixation would contribute dissolved inorganic nitrogen to Great Bay, which could in turn be immobilized within the sediment bed or assimilated by primary producers. Biotic assimilation would then contribute particulate and total nitrogen to the observed net export from Great Bay.

Dissolved organic carbon budget dynamics and net ecosystem metabolism

Temporal variability in DOC retention and export from Great Bay is influenced by the balance between primary production and ecosystem respiration, which drives the production and consumption of organic carbon. Positive net ecosystem metabolism rates indicate that autotrophic processes dominate and that organic matter is produced, whereas negative rates indicate heterotrophic processes dominate and organic matter is consumed faster than it is replaced (Odum, 1956; Seidensticker et al., 2019). The interannual variability in net ecosystem metabolism and carbon budgets in estuaries is linked, as DOC processing drives the balance

between autotrophic and heterotrophic status (Bauer et al., 2013; Windham-Myers et al., 2018) At a global scale, estuaries are categorized as heterotrophic, due to rates of respiration exceeding the combined supply of terrestrial organic carbon inputs and *in-situ* production (Bauer et al., 2013). A study of 42 sites within the National Estuarine Research Reserve system found that a majority (39) of the estuarine sites were net heterotrophic in a given year (Caffrey, 2004). Great Bay Estuary had a nearly balanced metabolism rate -0.2 ± 0.2 g O_2 m^{-2} day^{-1} across the five year study period (Caffrey, 2004). Given the standard error in Caffrey (2004), this result is similar to this study's findings that Great Bay fluctuates between autotrophic and heterotrophic status. One major difference between Caffrey (2004) and this study is that the tidal influence on the oxygen time series was removed to better capture the biological influence on net ecosystem metabolism. This methodology difference likely accounts for the narrower range in net ecosystem metabolism observed in this study.

Residence time, nutrient loading, and habitat type are all key controls of net ecosystem metabolism and consequently the balance of carbon (Caffrey, 2004; Hopkinson & Vallino, 1995). The longer a parcel of water remains in a system, the more time there is for nutrients and carbon to be selectively processed and retained (Hopkinson & Vallino, 1995; Howarth et al., 2006). In lower precipitation years, the reduction of freshwater inputs increases residence time, allowing primary producers to process more inorganic nutrient inputs and resulting in a net autotrophic system (Hopkinson & Vallino, 1995; Huang & Spaulding, 2002). For example, Great Bay was net autotrophic in the lowest precipitation year during the study period (979 mm total). Decreased freshwater inputs can also reduce nutrient loading from terrestrial sources (Seitzinger et al., 2005). While precipitation and discharge to Great Bay did not correlate with nitrogen or

carbon budget results, some of the lowest DIN input loads occurred in low precipitation and high primary productivity years.

Variability in the DOC Δ storage term indicates the consumption of terrestrial DOC inputs to Great Bay and the production of marine DOC within the estuary. Stable carbon isotope studies of the Mississippi River and Pearl River estuaries found that terrestrially-derived inputs of DOC are rapidly consumed within estuaries, resulting in the need for coastal ecosystems to supply additional autochthonous carbon (Wang et al., 2004; Ye et al., 2018). Three-fourths of terrestrial organic matter inputs from the Amazon River are estimated to be respired at the river delta (Hedges et al., 1997). The observation in the global carbon cycle that marine organic matter, including DOC, is usually not of terrestrial origins (Hedges et al., 1997) is supported by this study's observation of increasing respiration (more negative) with increasing DOC inputs to Great Bay.

Habitat type within Great Bay likely contributes to *in-situ* production of DOC. Caffrey (2004) found that estuary sites with submerged aquatic vegetation, either eelgrass or macroalgae, were more often net autotrophic or balanced. In Great Bay, as primary productivity increased, output of DOC from the system also increased, indicating additional *in-situ* production of organic matter. This may explain the observation of negative Δ storage values of DOC, where output exceeded inputs. DOC can be introduced to the water column from primary productivity during the desiccation of eelgrass (Vähätalo & Søndergaard, 2002; Penhale & Smith, 1977). Other estuarine systems, including the Mullica River – Great Bay Estuary (New Jersey) and the North Inlet Estuary (South Carolina), have demonstrated an annual net export of DOC to the coastal

ocean (Flynn, 2008; Williams et al., 1992). Overall, the flux between net export and net retention of DOC in Great Bay is likely the result of varying autotrophic and heterotrophic status.

Orthophosphate is retained in Great Bay

The sediment bed of Great Bay may be a net sink of orthophosphate, resulting in positive Δ storage values for the PO_4^{3-} black box model. Net retention of orthophosphate has been documented across a wide range of estuarine systems, including the Delaware Estuary (Lebo & Sharp, 1992), the Chesapeake Bay (Fisher et al., 1988), and the Hudson River Estuary (Fisher et al., 1988). Along the North American continental shelf, estuaries are estimated to retain between 10 and 55% of total phosphorus inputs from riverine fluxes (Nixon et al., 1996). A mass balance of orthophosphate in Delaware Bay shows similar patterns, with orthophosphate fluxes decreasing by more than 65% as water flows through the estuary and exits to the coastal ocean (Lebo & Sharp, 1992).

Often, retention of orthophosphate is observed in conjunction with increases in total phosphorus export, indicating a transformation of orthophosphate into particulate phosphate (Lebo & Sharp, 1992). The movement of phosphorus between dissolved and particulate fractions occurs with burial and biotic uptake of dissolved inorganic forms. Orthophosphate can become bound to iron oxides in estuarine sediments under aerobic conditions and buried within the sediment bed (Mort et al., 2010; Sulu-Gambari et al., 2018). Burial efficiency, the percentage of total phosphorus input at the sediment bed surface that is buried at least 10cm down, of reactive phosphorus (orthophosphate, organic phosphorus, and iron-bound phosphorus) ranged between 16 and 23% in Lake Grevelingen, a former estuary in the North Sea (Sulu-Gambari et al., 2018). Burial of

total phosphorus in the Patuxent River Estuary accounted for 61% of all total phosphorus inputs (Boynton et al., 2008). Great Bay is well mixed and well-oxygenated, with monthly average dissolved oxygen concentrations ranging from 7.65 mg L^{-1} in August to 10.7 mg L^{-1} in April (Appendix B, Figure B3). The oxic conditions in Great Bay and minimal evidence of orthophosphate release from resuspension of benthic sediments and from diffusive flux (Percuoco et al., 2015; Wengrove et al., 2015) support the conclusion of net orthophosphate burial driving positive Δ storage values.

As N:P ratios in Great Bay indicate N limitation in the summer, biotic uptake of phosphorus is a plausible explanation for the retention of orthophosphate. Estuarine systems typically have total N:P ratios that range between 10 and 20 (molar), thus falling close to the Redfield Ratio of 16:1 (Downing, 1997). Even with the observed wider N:P range in Great Bay, results are consistent with findings in Downing (1997), that estuaries fluctuate between N and P limitation. Median N:P ratios for inputs into Great Bay fall below the Redfield Ratio starting in July, indicating that N is the limiting nutrient in the summer and fall months, while P is limiting in the spring. Seasonal fluctuation between N and P limitation has been observed in the Chesapeake Bay, with phytoplankton being P limited in the spring and N limited in the summer (Malone et al., 1996). This switch is thought to be driven by temporal variation in whether growth-rates or biomass of phytoplankton is nutrient limited (Malone et al., 1996). Phytoplankton and macroalgae species (e.g., *Gracilaria)* outcompete rooted submerged aquatic vegetation for dissolved inorganic nutrients (Short et al., 1995; Valiela et al., 1997). In Waquoit Bay, macroalgal biomass accumulates in the warm summer months, when temperatures and light availability provide ideal growth conditions (Peckol et al., 1994). Consequently, these primary producers can rapidly

deplete dissolved inorganic nutrients from the water column and create a shift in N:P ratios. High primary productivity rates in the summer months of Great Bay support this theory.

Relationships between solute budgets and coastal management

Recently, several towns within the Great Bay Estuary watershed have made major improvements to their wastewater treatment facilities in an effort that should reduce nutrient loading inputs to Great Bay. In 2017, the Newmarket facility finished its upgrade to a four-stage Bardenpho system, which will help reduce its total nitrogen footprint on Great Bay Estuary. Both the Exeter wastewater treatment facility and the Portsmouth wastewater treatment facility also completed upgrades in 2020. It was assumed for this model that any wastewater treatment facility contributions upstream of Adams Point were represented in the high tide flux that travels from the Gulf of Maine, through the Piscataqua River and Little Bay, to Great Bay. As the box model only goes through 2018 currently, it is unclear whether these wastewater treatment upgrades have affected solute budgets.

Model limitations

It was difficult to elucidate the relationship between solute inputs to Great Bay and eelgrass health. Eelgrass coverage measured once a year at a broad scale (minimum 10% cover threshold) results in only a coarse description of eelgrass health each year. Calculation of solute inputs using continuous discharge and monthly grab samples captures more of the temporal variability in the ecosystem, including seasonal variation in the drivers of biogeochemical cycling (e.g., primary productivity). An important next step for this model is to estimate internal recycling and loss terms and attempt to fully balance the box model.

The lack of a linear relationship between eelgrass coverage and the box model results suggests that the relationship between eelgrass and nutrient loading is nonlinear, and may exhibit threshold behavior at nutrient levels present prior to the study period. Eelgrass has continued to decline in Great Bay, while DIN inputs, output, and Δ storage did not show strong temporal trends. Other studies have demonstrated that when nitrogen loads to coastal systems exceed a threshold of 50 kg N ha^{-1} $year^{-1}$, significant eelgrass decline occurs (Latimer & Rego, 2010; Valiela et al., 1997). DIN inputs to Great Bay have stayed above that threshold, and thus continue to be a stressor for eelgrass.

The comparison of concentrations across input and output terms provides an interesting, snapshot approach to understanding the balance between inputs and outputs in an estuarine system. The benefit of this approach is that estimates of tidal water fluxes are not necessary, assuming that high and low tide concentrations are not significantly different. In the case of Great Bay, input concentrations of DOC, DIN, and PO_4^{3-} exceeded estuarine tidal output concentrations (Table 2). This agreed with overall inter-annual observations of net retention for these solutes but did not capture deviations from the trend towards net exporter status (i.e., negative Δ storage). In instances where high and low tide concentrations were significantly different, Great Bay was a net exporter, which agreed with solute budget findings for TN and PN.

While the mean concentrations of TN and PN at high and low tide were statistically different, the overlap in the distributions due to the high standard deviations makes it difficult to definitively say that high tide concentrations are always higher than low tide concentrations. This

complicates the observation of net export of TN and PN from Great Bay, as riverine concentrations were higher than estuarine average concentrations. This does not necessarily indicate disagreement with the box model results though. The dilution calculation results indicated that it is not possible to detect the influence of riverine total nitrogen inputs on Great Bay at a decadal scale, likely due to the relatively small contribution of freshwater inputs (on average) to the estuary (~2%). Similarly, DIN concentrations from the freshwater rivers also dilute to undetectable levels in Great Bay at a decadal time step. If riverine inputs dilute to low concentrations in the estuary, it is entirely possible that internal production within the system makes up the difference, resulting in a net exporter status.

Despite the dilution of TN and DIN river contributions, the balance between net export of TN and net import of DIN can be partly explained through the wastewater treatment effluent inputs. The calculation that freshwater inputs, on a decadal average, comprise 2% of the estuary's tidal prism (Trowbridge, 2007), did not include wastewater treatment effluent. Thus, the three wastewater treatment facilities included in this box model contribute additional water and nitrogen to the system. As this effluent is mostly DIN (84%), it indicates that Great Bay was receiving a high input of DIN from this source and relatively little additional TN. Consequently, Great Bay was receiving enough DIN to import and use and an insufficient amount of TN, resulting in additional production within the estuary. The uptake of DIN within Great Bay is further supported by the flip from phosphorus to nitrogen limitation, shown in the N:P ratios of this study.

This difference, between concentration observations and load results, highlights the difficulty in resolving a temporally complex data set for a system influenced by daily tidal fluctuations and extreme weather events. Estuaries are ecosystems where the river meets the sea – indicating the mixing of fresh and salt water. Salinity levels in estuaries have been shown to decrease with increasing freshwater input (Regnier et al., 2013) and variability in freshwater input influences the rate of delivery for terrestrial solutes (Eyre & Balls, 1999). This is consistent with the results for Great Bay, with salinity levels decreasing as freshwater discharge to the system increases (Figure B5). Nitrate concentrations have been shown to decrease as water moves along the estuarine gradient (Valiela et al., 2021). Estuarine nutrient concentrations tend to dilute as freshwater rich in nitrogen mixes with nitrogen-poor salt water (Valiela et al., 2021). This is the case in Great Bay, where TN and DIN river concentrations dilute to undetectable concentration levels at a decadal time-step. Yet, as river discharge increases, observed low tide concentrations in DIN, PN, and TN increase (Figure 3). PN had a smaller slope than DIN or TN in relation to freshwater input, suggesting that river input of PN was either not captured at a monthly grab sampling time step or that PN inputs from rivers are lower than DIN inputs.

Consideration of the dilution effect helps to clarify how river concentrations can be higher than estuarine concentrations, while box model results indicate the opposite (with inputs less than outputs). While at a decadal scale, nitrogen river inputs appear to dilute to negligible concentrations, daily and annual time steps suggest that the river inputs do enrich estuarine concentrations at higher freshwater flow events. These opposing observations are likely due to differences in temporal resolution, with the decadal dilution calculations smoothing out temporal variability in concentration data. When daily and annual time-steps are examined, discrete

weather events such as storms can increase the rate of delivery of terrestrial solutes to an estuary and the rate of flushing out on an estuary (Geyer et al., 2018). While it is important to recognize the limitations of a concentration perspective, this approach can be a useful tool in quickly assessing biogeochemical inputs and outputs when the hydrodynamics of a system are not fully quantified. A fully quantified hydrodynamic model would increase confidence in estuarine flux estimates both into and out of Great Bay, by allowing for a more sensitive tidal prism estimate that varied daily.

Given the wide range in uncertainty in the Δ storage terms for each solute, there is a possibly that some of the storage terms in individual years could switch between export and import interpretations. The wide range in uncertainty for calculated Δ storage terms (Appendix A, Table A4) is likely due to a combination of the propagation of error terms as inputs and outputs were summed and subtracted and the differences in resolution of measurement across terms. The high variability in Δ storage estimates between years for each solute, likely contributes to the wide range of uncertainty. By looking at the lowest and highest input and output years, a wider range of uncertainty is calculated than what is observed in the range of annual Δ storage estimates. The low standard error of individual input terms supports the idea that the wider uncertainty range in the storage estimates originates from the calculation of Δ storage. Boynton et al. (2008) notes that uncertainty associated with tidal transport is difficult and often beyond the current capability of modeling methods. This is seen in Great Bay, where the tidal prism estimate is reported with no range of variability or error. The tidal inputs and outputs to this system were the largest of the terms used in the box model, suggesting that the high uncertainty in Δ storage terms may also be due to the high uncertainty in tidal flux.

CHAPTER 5: CONCLUSION

A mass balance, black box modeling approach is a useful tool for understanding how estuarine biogeochemical cycles vary with solute type and relative input load. Model results for all solutes showed non-conservative behavior, meaning solutes were either transformed and retained in Great Bay and/or produced. Of particular interest is the contrast between the behavior of particulate and dissolved forms of nutrients. On a decadal and annual scale, Great Bay is a net export of total nitrogen, particulate nitrogen, and total suspended solids, but a net importer of dissolved nutrients and carbon. This difference across forms of nutrients demonstrates the influence of biological drivers on biogeochemical cycling in estuaries. The balance between primary production and ecosystem respiration and the balance between phosphorus and nitrogen limitation in Great Bay helps to explain the net retention of dissolved forms of nutrients and carbon. As primary producers and the microbial community uptake dissolved nitrogen, phosphorus, and carbon, these solutes are incorporated in particulate forms and can subsequently contribute to the net export of particulate matter.

While biogeochemical stressor and ecological response relationships were not obvious with changes in eelgrass coverage, net storage of DIN may provide an indirect explanation. The eutrophication of estuaries, like Great Bay, often drives high rates of primary productivity, as nitrogen limitations are temporarily reduced. With sufficient nitrogen, primary producers are no longer limited by a lack of nutrients. Growth of phytoplankton and macroalgae would explain continued storage of DIN in Great Bay in the face of growing eelgrass decline and could create light limitation for the rooted SAV species. Future work should explore whether DIN storage in Great Bay relates to macroalgal biomass and coverage.

In terms of management, the interpretation of Δ storage values depends on the question being asked. Positive DIN storage values for Great Bay indicate a net import of nutrients into the ecosystem, which can be explained by a combination of inputs from wastewater treatment plants in the region and non-point source contributions. In this context, the high amount of DIN input could be considered a stressor to the ecosystem, contributing to nutrient-stimulated light attenuation by macrophytes. Positive DIN storage values can also be considered in the context of ecological processes, such as the nutrient needs of the ecological community (i.e., eelgrass, phytoplankton, etc.) and rates of permanent removal through denitrification. In this context, DIN inputs may not be a stressor but rather contribute to the nitrogen needs of the primary producer community. In this instance, positive storage values would simply reflect the ecosystem responding to the influx of nutrients with additional production of biomass. The key difference between these interpretations is whether there is evidence of eutrophication in the ecosystem in question. In the case of Great Bay, declines in eelgrass, combined with increases in macroalgae, suggest nutrient inputs may be doing more harm than good.

LIST OF REFERENCES

Alvarez-Fernandez, S., & Riegman, R. (2014). Chlorophyll in North Sea coastal and offshore waters does not reflect long term trends of phytoplankton biomass. *Journal of Sea Research, 91*, 35–44. https://doi.org/10.1016/j.seares.2014.04.005

Aoki, L. R., & McGlathery, K. J. (2017). Push-pull incubation method reveals the importance of denitrification and dissimilatory nitrate reduction to ammonium in seagrass root zone. *Limnology and Oceanography: Methods*, *15*(9), 766–781. https://doi.org/10.1002/lom3.10197

Aoki, L. R., McGlathery, K. J., & Oreska, M. P. J. (2020). Seagrass restoration reestablishes the coastal nitrogen filter through enhanced burial. *Limnology and Oceanography*, *65*(1), 1–12. https://doi.org/10.1002/lno.11241

Bach, S. D., Thayer, G. W., & LaCroix, M. W. (1986). Export of detritus from eelgrass (Zostera marina) beds near Beaufort, North Carolina, USA. *Marine Ecology Progress Series*, *28*(3), 265–278. https://www.jstor.org/stable/24817444

Baird, D., Winter, P. E. D., & Wendt, G. (1987). The flux of particulate material through a well-mixed estuary. *Continental Shelf Research*, *7*(11–12), 1399–1403.

Ballestero, T. P., Roseen, R., & Brannaka, L. K. (2004). Inflow and Loadings from Ground Water to the Great Bay Estuary, New Hampshire. *PREP Reports & Publications*, 127.

Barbier, E. B., Hacker, S. D., Kennedy, C., Koch, E. W., Stier, A. C., & Silliman, B. R. (2011). The value of estuarine and coastal ecosystem services. *Ecological Monographs*, *81*(2), 169–193. https://doi.org/10.1890/10-1510.1

Barker, S. (2018). *Eelgrass Distribution in the Great Bay Estuary and Piscataqua River for 2017* (No. 407; p. 38). PREP Reports & Publications. https://scholars.unh.edu/prep/407

Barker, S. (2020). *Eelgrass Distribution in the Great Bay Estuary and Piscataqua River for 2019: Final Project Report submitted to the Piscataqua Region Estuaries Partnership* (No. 438; p. 40). PREP Reports & Publications. https://scholars.unh.edu/prep/438

Bauer, J. E., Cai, W.-J., Raymond, P. A., Bianchi, T. S., Hopkinson, C. S., & Regnier, P. A. G. (2013). The changing carbon cycle of the coastal ocean. *Nature*, *504*(7478), 61–70. https://doi.org/10.1038/nature12857

Bell, S., & Hall, M. (1997). Drift macroalgal abundance in seagrass beds:investigating large-scale associations with physical and biotic attributes. *Marine Ecology Progress Series*, *147*, 277–283. https://doi.org/10.3354/meps147277

Bilgili, A., Proehl, J., Lynch, D., Smith, K., & Swift, M. (2005). Estuary/ocean exchange and tidal mixing in a Gulf of Maine Estuary: A Lagrangian modeling study. *Estuarine, Coastal and Shelf Science*, *65*, 607–624. https://doi.org/10.1016/j.ecss.2005.06.027

Bowen, J. L., & Valiela, I. (2008). Using [delta]^sup 15^N to Assess Coupling between Watersheds and Estuaries in Temperate and Tropical Regions. *Journal of Coastal Research; Fort Lauderdale*, *24*(3), 804–813. https://search.proquest.com/docview/210844236/abstract/2F754231B17D42EFPQ/1

Boynton, W. R., Garber, J. H., Summers, R., & Kemp, W. M. (1995). Inputs, transformations, and transport of nitrogen and phosphorus in Chesapeake Bay and selected tributaries. *Estuaries*, *18*(1), 285–314. https://doi.org/10.2307/1352640

Boynton, W. R., Hagy, J. D., Cornwell, J. C., Kemp, W. M., Greene, S. M., Owens, M. S., Baker, J. E., & Larsen, R. K. (2008). Nutrient Budgets and Management Actions in the Patuxent River Estuary, Maryland. *Estuaries and Coasts*, *31*(4), 623–651. https://doi.org/10.1007/s12237-008-9052-9

Bukaveckas, P. A., Beck, M., Devore, D., & Lee, W. M. (2018). Climatic variability and its role in regulating C, N and P retention in the James River Estuary. *Estuarine, Coastal and Shelf Science*, *205*, 161–173. https://doi.org/10.1016/j.ecss.2017.10.004

Burdick, D., Edwardson, K., Gregory, T., Matso, K., Mattera, T., Paly, M., Peter, C., Short, F., & Torio, D. (2020). *A Case for Restoration and Recovery of Zostera marina L. in the Great Bay Estuary* (No. 441; p. 28). https://www.greatbay.org/wp-content/uploads/2020/05/Seagrass-White-Paper-FINAL-May-8-2020.pdf

Burdick, D. M., Moore, G. E., Mathieson, A. C., Payne, A., & Peter, C. (2019). Macroalgal Monitoring in the Great Bay Estuary: 2018 Annual Report. *PREP Reports & Publications*, 34. https://scholars.unh.edu/cgi/viewcontent.cgi?article=1430&context=prep

Burdick, D., Mathieson, A. C., Nick, S., McGovern, M., & Peter, C. R. (2017). Monitoring Macroalgae in the Great Bay Estuary for 2016. *PREP Reports & Publications*, 32. https://www.stateofourestuaries.org/wp-content/uploads/2018/06/Monitoring-Macroalgae-in-the-Great-Bay-Estuary-for-2016.pdf

Buzzelli, C., Wan, Y., Doering, P. H., & Boyer, J. N. (2013). Seasonal dissolved inorganic nitrogen and phosphorus budgets for two sub-tropical estuaries in south Florida, USA. *Biogeosciences; Katlenburg-Lindau*, *10*(10), 6721. http://dx.doi.org/10.5194/bg-10-6721-2013

Caffrey, J. M. (2004). Factors controlling net ecosystem metabolism in U.S. estuaries. *Estuaries*, *27*(1), 90–101. https://doi.org/10.1007/BF02803563

Cai, W.-J., & Wang, Y. (1998). The chemistry, fluxes, and sources of carbon dioxide in the estuarine waters of the Satilla and Altamaha Rivers, Georgia. *Limnology and Oceanography*, *43*(4), 657–668. https://doi.org/10.4319/lo.1998.43.4.0657

Capone, D. G. (1982). Nitrogen Fixation (Acetylene Reduction) by Rhizosphere Sediments of the Eelgrass Zostera marina. *Marine Ecology Progress Series*, *10*(1), 67–75. https://www.jstor.org/stable/24815015

Chalifour, L., Scott, D., MacDuffee, M., Iacarella, J., Martin, T., & Baum, J. (2019). Habitat use by juvenile salmon, other migratory fish, and resident fish species underscores the importance of estuarine habitat mosaics. *Marine Ecology Progress Series*, *625*, 145–162. https://doi.org/10.3354/meps13064

Cole, L., & McGlathery, K. (2012). Nitrogen fixation in restored eelgrass meadows. *Marine Ecology Progress Series*, *448*, 235–246. https://doi.org/10.3354/meps09512

Cook, S. (2019). Effects of Waves, Tides, and Vegetation on the Distribution of Bed Shear Stress in the Great Bay Estuary, NH. *Doctoral Dissertations 2485*. https://scholars.unh.edu/dissertation/2485

de Boer, W. F. (2007). Seagrass–sediment interactions, positive feedbacks and critical thresholds for occurrence: A review. *Hydrobiologia*, *591*(1), 5–24. https://doi.org/10.1007/s10750-007-0780-9

DeSimone, L. A., & Howes, B. L. (1998). Nitrogen transport and transformations in a shallow aquifer receiving wastewater discharge: A mass balance approach. *Water Resources Research*, *34*(2), 271–285. https://doi.org/10.1029/97WR03040

Diaz, R., & Rosenberg, R. (2008). Spreading Dead Zones and Consequences for Marine Ecosystems. *Science*, *321*, 926–929. https://doi.org/10.1126/science.1156401

Downing, J. A. (1997). Marine Nitrogen: Phosphorus Stoichiometry and the Global N:P Cycle. *Biogeochemistry*, *37*(3), 237–252. https://www.jstor.org/stable/1468990

Duarte, C. M., Dennison, W. C., Orth, R. J. W., & Carruthers, T. J. B. (2008). The Charisma of Coastal Ecosystems: Addressing the Imbalance. *Estuaries and Coasts*, *31*(2), 233–238. https://doi.org/10.1007/s12237-008-9038-7

Eyre, B., & Balls, P. (1999). A comparative study of nutrient behavior along the salinity Gradient of tropical and temperate estuaries. *Estuaries*, *22*(2), 313–326. https://doi.org/10.2307/1352987

Eyre, B. D., Maher, D. T., & Sanders, C. (2016). The contribution of denitrification and burial to the nitrogen budgets of three geomorphically distinct Australian estuaries: Importance of seagrass habitats. *Limnology and Oceanography*, *61*(3), 1144–1156. https://doi.org/10.1002/lno.10280

Feng, Y., Friedrichs, M. A. M., Wilkin, J., Tian, H., Yang, Q., Hofmann, E. E., Wiggert, J. D., & Hood, R. R. (2015). Chesapeake Bay nitrogen fluxes derived from a land-estuarine ocean biogeochemical modeling system: Model description, evaluation, and nitrogen budgets. *Journal of Geophysical Research: Biogeosciences*, *120*(8), 1666–1695. https://doi.org/10.1002/2015JG002931

Fisher, T. R., Harding, L. W., Stanley, D. W., & Ward, L. G. (1988). Phytoplankton, nutrients, and turbidity in the Chesapeake, Delaware, and Hudson estuaries. *Estuarine, Coastal and Shelf Science*, *27*(1), 61–93. https://doi.org/10.1016/0272-7714(88)90032-7

Flynn, A. M. (2008). Organic Matter and Nutrient Cycling in a Coastal Plain Estuary: Carbon, Nitrogen, and Phosphorus Distributions, Budgets, and Fluxes. *Journal of Coastal Research; Fort Lauderdale*, *SI*(55), 76–94. https://search.proquest.com/docview/1673541589/abstract/157C272BDE74F7APQ/1

Fonseca, M. S., & Cahalan, J. A. (1992). A preliminary evaluation of wave attenuation by four species of seagrass. *Estuarine, Coastal and Shelf Science*, *35*(6), 565–576. https://doi.org/10.1016/S0272-7714(05)80039-3

Fourqurean, J. W., Duarte, C. M., Kennedy, H., Marbà, N., Holmer, M., Mateo, M. A., Apostolaki, E. T., Kendrick, G. A., Krause-Jensen, D., McGlathery, K. J., & Serrano, O. (2012). Seagrass ecosystems as a globally significant carbon stock. *Nature Geoscience*, *5*(7), 505–509. https://doi.org/10.1038/ngeo1477

Freeman, L. A., Corbett, D. R., Fitzgerald, A. M., Lemley, D. A., Quigg, A., & Steppe, C. N. (2019). Impacts of Urbanization and Development on Estuarine Ecosystems and Water Quality. *Estuaries and Coasts*, *42*(7), 1821–1838. https://doi.org/10.1007/s12237-019-00597-z

Ganju, N. K., Miselis, J. L., & Aretxabaleta, A. L. (2014). Physical and biogeochemical controls on light attenuation in a eutrophic, back-barrier estuary. *Biogeosciences*, *11*(24), 7193–7205. https://doi.org/10.5194/bg-11-7193-2014

Geyer, N., Huettel, M., & Wetz, M. (2018). Biogeochemistry of a River-Dominated Estuary Influenced by Drought and Storms. *Estuaries and Coasts*, *41*(7), 2009–2023. https://doi.org/10.1007/s12237-018-0411-x

Hansen, J. C. R., & Reidenbach, M. A. (2013). Seasonal Growth and Senescence of a Zostera marina Seagrass Meadow Alters Wave-Dominated Flow and Sediment Suspension Within a Coastal Bay. *Estuaries and Coasts*, *36*(6), 1099–1114. https://doi.org/10.1007/s12237-013-9620-5

Hedges, J. I., Keil, R. G., & Benner, R. (1997). What happens to terrestrial organic matter in the ocean? *Organic Geochemistry*, *27*(5), 195–212. https://doi.org/10.1016/S0146-6380(97)00066-1

Hemminga, M. A., Harrison, P. G., & Lent, F. van. (1991). The balance of nutrient losses and gains in seagrass meadows. *Marine Ecology Progress Series*, *71*, 85–96. https://www.int-res.com/articles/meps/71/m071p085.pdf

Hill, K. A., Shepson, P. B., Galbavy, E. S., & Anastasio, C. (2005). Measurement of wet deposition of inorganic and organic nitrogen in a forest environment. *Journal of Geophysical Research: Biogeosciences*, *110*(G2). https://doi.org/10.1029/2005JG000030

Hopkinson, C. S., & Vallino, J. J. (1995). The Relationships among Man's Activities in Watersheds and Estuaries: A Model of Runoff Effects on Patterns of Estuarine Community Metabolism. *Estuaries*, *18*(4), 598. https://doi.org/10.2307/1352380

Howarth, R., Swaney, D., Boyer, E., Marino, R., Jaworski, N., & Goodale, C. (2006). The influence of climate on average nitrogen export from large watersheds in the Northeastern United States. *Biogeochemistry*, *79*(1–2), 163–186. http://dx.doi.org.unh.idm.oclc.org/10.1007/s10533-006-9010-1

Huang, W., & Spaulding, M. (2002). Modelling residence-time response to freshwater input in Apalachicola Bay, Florida, USA. *Hydrological Processes*, *16*(15), 3051–3064. https://doi.org/10.1002/hyp.1088

Iizumi, H., Hattori, A., & McRoy, C. P. (1980). Nitrate and nitrite in interstitial waters of eelgrass beds in relation to the rhizosphere. *Journal of Experimental Marine Biology and Ecology*, *47*(2), 191–201. https://doi.org/10.1016/0022-0981(80)90112-4

Kirk, J. (1983). *Light and photosynthesis in aquatic ecosystems* (1st ed.). Cambridge University Press.

Lacy, J. R., & Wyllie-Echeverria, S. (2011). The influence of current speed and vegetation density on flow structure in two macrotidal eelgrass canopies. In *Limnology and Oceanography: Fluids and Environments* (Vol. 1, Issue 2011, p. 3855). https://doi.org/10.1215/21573698-1152489

Laruelle, G. G., Dürr, H. H., Lauerwald, R., Hartmann, J., Slomp, C. P., Goossens, N., & Regnier, P. A. G. (2013). Global multi-scale segmentation of continental and coastal waters from the watersheds to the continental margins. *Hydrology and Earth System Sciences*, *17*(5), 2029–2051. https://doi.org/10.5194/hess-17-2029-2013

Latimer, J. S., & Rego, S. A. (2010). Empirical relationship between eelgrass extent and predicted watershed-derived nitrogen loading for shallow New England estuaries. *Estuarine, Coastal and Shelf Science*, *90*(4), 231–240. https://doi.org/10.1016/j.ecss.2010.09.004

Lebo, M. E., & Sharp, J. H. (1992). Modeling phosphorus cycling in a well-mixed coastal plain estuary. *Estuarine, Coastal and Shelf Science*, *35*(3), 235–252. https://doi.org/10.1016/S0272-7714(05)80046-0

Lehrter, J. C., & Cebrian, J. (2010). Uncertainty propagation in an ecosystem nutrient budget. *Ecological Applications*, *20*(2), 508–524. http://www.jstor.org/stable/27797824

Liptzin, D., Daley, M. L., & McDowell, W. H. (2013). A Comparison of Wet Deposition Collectors at a Coastal Rural Site. *Water, Air, & Soil Pollution*, *224*(5). https://doi.org/10.1007/s11270-013-1558-5

Malone, T. C., Conley, D. J., Fisher, T. R., Glibert, P. M., Harding, L. W., & Sellner, K. G. (1996). Scales of nutrient-limited phytoplankton productivity in Chesapeake Bay. *Estuaries*, *19*(2), 371–385. https://doi.org/10.2307/1352457

Matso, K., & Potter, J. (2018). Great Bay Estuary Tidal Tributary Monitoring Program: Quality Assurance Project Plan, 2018. *PREP Reports & Publications*. https://scholars.unh.edu/prep/406

McGlathery, K., Risgaard-Petersen, N., & Christensen, P. (1998). Temporal and spatial variation in nitrogen fixation activity in the eelgrass Zostera marina rhizosphere. *Marine Ecology Progress Series*, *168*, 245–258. https://doi.org/10.3354/meps168245

Mort, H. P., Slomp, C. P., Gustafsson, B. G., & Andersen, T. J. (2010). Phosphorus recycling and burial in Baltic Sea sediments with contrasting redox conditions. *Geochimica et Cosmochimica Acta*, *74*(4), 1350–1362. https://doi.org/10.1016/j.gca.2009.11.016

Neff, J. C., Holland, E. A., Dentener, F. J., McDowell, W. H., & Russell, K. M. (2002). The origin, composition and rates of organic nitrogen deposition: A missing piece of the nitrogen cycle? In E. W. Boyer & R. W. Howarth (Eds.), *The Nitrogen Cycle at Regional to Global Scales* (pp. 99–136). Springer Netherlands. https://doi.org/10.1007/978-94-017-3405-9_3

Nixon, S. W., Ammerman, J. W., Atkinson, L. P., Berounsky, V. M., Billen, G., Boicourt, W. C., Boynton, W. R., Church, T. M., Ditoro, D. M., Elmgren, R., Garber, J. H., Giblin, A. E., Jahnke, R. A., Owens, N. J. P., Pilson, M. E. Q., & Seitzinger, S. P. (1996). The fate of nitrogen and phosphorus at the land-sea margin of the North Atlantic Ocean. *Biogeochemistry*, *35*(1), 141–180. https://doi.org/10.1007/BF02179826

Odebrecht, C., Abreu, P. C., & Carstensen, J. (2015). Retention time generates short-term phytoplankton blooms in a shallow microtidal subtropical estuary. *Estuarine, Coastal and Shelf Science*, *162*, 35–44. https://doi.org/10.1016/j.ecss.2015.03.004

Odum. (1980). The Status of Three Ecosystem-Level Hypotheses Regarding Salt Marsh Estuaries: Tidal Subsidy, Outwelling, and Detritus-Based Food Chains. In *Estuarine Perspectives* (pp. 485–495).

Odum, H. T. (1956). Primary Production in Flowing Waters1. *Limnology and Oceanography*, *1*(2), 102–117. https://doi.org/10.4319/lo.1956.1.2.0102

Oreska, M. P. J., McGlathery, K. J., & Porter, J. H. (2017). Seagrass blue carbon spatial patterns at the meadow-scale. *PLOS ONE*, *12*(4), e0176630. https://doi.org/10.1371/journal.pone.0176630

Peckol, P., DeMeo-Anderson, B., Rivers, J., Valiela, I., Maldonado, M., & Yates, J. (1994). Growth, nutrient uptake capacities and tissue constituents of the macroalgae Cladophora vagabunda and Gracilaria tikvahiae related to site-specific nitrogen loading rates. *Marine Biology*, *121*(1), 175–185. https://doi.org/10.1007/BF00349487

Pedersen, M. F., & Borum, J. (1993). An annual nitrogen budget for a seagrass Zostera marina population. *Marine Ecology Progress Series*, *101*(1/2), 169–177. https://www.jstor.org/stable/24840607

Penhale, P. A., & Smith, W. O. (1977). Excretion of dissolved organic carbon by eelgrass (Zostera marina) and its epiphytes1. *Limnology and Oceanography*, *22*(3), 400–407. https://doi.org/10.4319/lo.1977.22.3.0400

Percuoco, V. P., Kalnejais, L. H., & Officer, L. V. (2015). Nutrient release from the sediments of the Great Bay Estuary, N.H. USA. *Estuarine, Coastal and Shelf Science*, *161*, 76–87. https://doi.org/10.1016/j.ecss.2015.04.006

Piscataqua Region Estuaries Partnership. (2012). *Final Environmental Data Report December 2012: Technical Support Document for the 2013 State of Our Estuaries Report* (No. 265). PREP Reports & Publications.

Piscataqua Region Estuaries Partnership. (2017). *Final Environmental Data Report December 2017: Technical Support Document for the 2018 State of Our Estuaries Report.* (No. 383). PREP Reports & Publications. https://www.stateofourestuaries.org/2018-reports/data-report/

Piscataqua Region Estuaries Partnership. (2018). *State of Our Estuaries 2018*. stateofourestauries.org

Regnier, P., Arndt, S., Goossens, N., Volta, C., Laruelle, G. G., Lauerwald, R., & Hartmann, J. (2013). Modelling Estuarine Biogeochemical Dynamics: From the Local to the Global Scale. *Aquatic Geochemistry*, *19*(5), 591–626. https://doi.org/10.1007/s10498-013-9218-3

Reidenbach, M. A., & Thomas, E. L. (2018). Influence of the Seagrass, Zostera marina, on Wave Attenuation and Bed Shear Stress Within a Shallow Coastal Bay. *Frontiers in Marine Science*, *5*. https://doi.org/10.3389/fmars.2018.00397

Risgaard-Petersen, N., Dalsgaard, T., Rysgaard, S., Christensen, P. B., Borum, J., McGlathery, K., & Nielsen, L. P. (1998). Nitrogen balance of a temperate eelgrass Zostera marina bed. *Marine Ecology Progress Series*, *174*, 281–291. https://doi.org/10.3354/meps174281

Robertson, B. P., & Savage, C. (2021). Thresholds in catchment nitrogen load for shifts from seagrass to nuisance macroalgae in shallow intertidal estuaries. *Limnology and Oceanography*, *66*(4), 1353–1366. https://doi.org/10.1002/lno.11689

Sarma, V. V. S. S., Krishna, M. S., Prasad, V. R., Kumar, B. S. K., Naidu, S. A., Rao, G. D., Viswanadham, R., Sridevi, T., Kumar, P. P., & Reddy, N. P. C. (2014). Distribution and sources of particulate organic matter in the Indian monsoonal estuaries during monsoon. *Journal of Geophysical Research: Biogeosciences*, *119*(11), 2095–2111. https://doi.org/10.1002/2014JG002721

Seidensticker, L. E., Najjar, R. G., Herrmann, M., Boyer, J. N., Briceño, H. O., Kemp, W. M., & Tomaso, D. J. (2019). Seasonal and Interannual Variability in Net Ecosystem Production of a Subtropical Coastal Lagoon Inferred from Monthly Oxygen Surveys. *Estuaries and Coasts*, *42*(2), 455–469. https://doi.org/10.1007/s12237-018-0482-8

Seitzinger, Harrison, J. A., Böhlke, J. K., Bouwman, A. F., Lowrance, R., Peterson, B., Tobias, C., & Drecht, G. V. (2006). Denitrification Across Landscapes and Waterscapes: A Synthesis. *Ecological Applications*, *16*(6), 2064–2090. https://doi.org/10.1890/1051-0761(2006)016[2064:DALAWA]2.0.CO;2

Seitzinger, S. P., Harrison, J. A., Dumont, E., Beusen, A. H. W., & Bouwman, A. F. (2005). Sources and delivery of carbon, nitrogen, and phosphorus to the coastal zone: An overview of Global Nutrient Export from Watersheds (NEWS) models and their application. *Global Biogeochemical Cycles*, *19*(4). https://doi.org/10.1029/2005GB002606

Short, F. T. (Ed.). (1992). *The ecology of the Great Bay Estuary, New Hampshire and Maine: An Estuarine Profile and Bibliography*. 241.

Short, F. T. (2016). *Eelgrass Distribution and Biomass in the Great Bay Estuary for 2015* (No. 354; p. 6). PREP Reports & Publications. https://scholars.unh.edu/prep/354

Short, F. T., Burdick, D. M., & Kaldy, J. E. (1995). Mesocosm experiments quantify the effects of eutrophication on eelgrass, Zostera marina. *Limnology and Oceanography*, *40*(4), 740–749. https://doi.org/10.4319/lo.1995.40.4.0740

Smyth, A. R., Thompson, S. P., Siporin, K. N., Gardner, W. S., McCarthy, M. J., & Piehler, M. F. (2013). Assessing Nitrogen Dynamics Throughout the Estuarine Landscape. *Estuaries and Coasts*, *36*(1), 44–55. JSTOR. https://www.jstor.org/stable/23326685

Sulu-Gambari, F., Hagens, M., Behrends, T., Seitaj, D., Meysman, F. J. R., Middelburg, J., & Slomp, C. P. (2018). Phosphorus Cycling and Burial in Sediments of a Seasonally Hypoxic Marine Basin. *Estuaries and Coasts*, *41*(4), 921–939. https://doi.org/10.1007/s12237-017-0324-0

Takasu, H., Uchino, K., & Mori, K. (2020). Dissolved and Particulate Organic Matter Dynamics Relative to Sediment Resuspension Induced by the Tidal Cycle in Macrotidal Estuaries, Kyushu, Japan. *Water*, *12*, 2561. https://doi.org/10.3390/w12092561

Thursby, G. B., & Harlin, M. M. (1982). Leaf-root interaction in the uptake of ammonia by Zostera marina. *Marine Biology*, *72*(2), 109–112. https://doi.org/10.1007/BF00396910

Town of Exeter. (2019). *Total Nitrogen Control Plan Annual Report For 2019*. Town of Exeter. https://www.exeternh.gov/sites/default/files/fileattachments/public_works/page/38381/2019-exeter-tn-annual_report-20200131-final.pdf

Trowbridge, P. (2007). Hydrological Parameters for New Hampshire's Estuaries. *PREP Reports & Publications*. https://scholars.unh.edu/prep/130

Vähätalo, A. V., & Søndergaard, M. (2002). Carbon transfer from detrital leaves of eelgrass (Zostera marina) to bacteria. *Aquatic Botany*, *73*(3), 265–273. https://doi.org/10.1016/S0304-3770(02)00037-2

Valiela, I., Lloret, J., Chenoweth, K., Elmstrom, E., & Hanacek, D. (2021). Control of N Concentrations in Cape Cod Estuaries by Nitrogen Loads, Season, and Down-Estuary Transit: Assessment by Conventional and Effect-Size Statistics. *Estuaries and Coasts*, *44*(5), 1294–1309. https://doi.org/10.1007/s12237-020-00869-z

Valiela, I., McClelland, J., Hauxwell, J., Behr, P. J., Hersh, D., & Foreman, K. (1997). Macroalgal blooms in shallow estuaries: Controls and ecophysiological and ecosystem consequences. *Limnology and Oceanography*, *42*, 1105–1118. https://doi.org/10.4319/lo.1997.42.5_part_2.1105

Wang, X.-C., Chen, R. F., & Gardner, G. B. (2004). Sources and transport of dissolved and particulate organic carbon in the Mississippi River estuary and adjacent coastal waters of the northern Gulf of Mexico. *Marine Chemistry*, *89*(1), 241–256. https://doi.org/10.1016/j.marchem.2004.02.014

Welsh, D., Castadelli, G., Bartoli, M., Poli, D., Careri, M., de Wit, R., & Viaroli, P. (2001). Denitrification in an intertidal seagrass meadow, a comparison of 15N-isotope and acetylene-block techniques: Dissimilatory nitrate reduction to ammonia as a source of N2O? *Marine Biology*, *139*(6), 1029–1036. https://doi.org/10.1007/s002270100672

Wengrove, M., Foster, D., Kalnejais, L., Percuoco, V. P., & Lippmann, T. (2015). Field and laboratory observations of bed stress and associated nutrient release in a tidal estuary. *Estuarine, Coastal and Shelf Science*, *161*, 11–24.

Wild-Allen, K., & Andrewartha, J. (2016). Connectivity between estuaries influences nutrient transport, cycling and water quality. *Marine Chemistry*, *185*, 12–26. https://doi.org/10.1016/j.marchem.2016.05.011

Williams, T. M., Wolaver, T. G., Dame, R. F., & Spurrier, J. D. (1992). The Bly Creek ecosystem study—Organic carbon transport within a euhaline salt marsh basin, North Inlet, South Carolina. *Journal of Experimental Marine Biology and Ecology*, *163*(1), 125–139. https://doi.org/10.1016/0022-0981(92)90151-Y

Windham-Myers, L., Cai, W.-J., Alin, S., Andersson, A., Crosswell, J., Dunton, K. H., Hernandez-Ayon, J. M., Herrmann, M., Hinson, A. L., Hopkinson, C. S., Howard, J., Hu, X., Knox, S. H., Kroeger, K., Lagomasino, D., Megonigal, P., Najjar, R., Paulsen, M.-L., Peteet, D., … Zhu, Z. (2018). *Chapter 15: Tidal Wetlands and Estuaries. Second State of the Carbon Cycle Report*. U.S. Global Change Research Program. https://doi.org/10.7930/SOCCR2.2018.Ch15

Winter, P. E. D., Schlacherl, T. A., & Baird, D. (1996). Carbon flux between an estuary and the ocean: A case for outwelling. *Hydrobiologia*, *337*(1–3), 123–132. https://doi.org/10.1007/BF00028513

Wollast, R. (1983). Interactions in Estuaries and Coastal Waters. In B. Bolin & R. B. Cook (Eds.), *The Major Biogeochemical Cycles and Their Interactions* (pp. 385–407). Wiley.

Ye, F., Guo, W., Wei, G., & Jia, G. (2018). The Sources and Transformations of Dissolved Organic Matter in the Pearl River Estuary, China, as Revealed by Stable Isotopes. *Journal of Geophysical Research: Oceans*, *123*(9), 6893–6908. https://doi.org/10.1029/2018JC014004

Young, M., Gonneea, M. E., Herrera-Silveira, J., & Paytan, A. (2005). Export of Dissolved and Particulate Carbon and Nitrogen From a Mangrove-Dominated Lagoon, Yucatan Peninsula, Mexico. *International Journal of Ecology and Environmental Sciences*, *31*(3), 189–202.

Zhang, J., Lei, J., Huai, W., & Nepf, H. (2020). Turbulence and Particle Deposition Under Steady Flow Along a Submerged Seagrass Meadow. *Journal of Geophysical Research: Oceans*, *125*(5), e2019JC015985. https://doi.org/10.1029/2019JC015985

Zuo, J., Song, J., Yuan, H., Li, X., Li, N., & Duan, L. (2016). Particulate nitrogen and phosphorus in the East China Sea and its adjacent Kuroshio waters and evaluation of budgets for the East China Sea Shelf. *Continental Shelf Research*, *131*, 1–11. https://doi.org/10.1016/j.csr.2016.11.003

.

TABLES

Table 1. Average solute concentrations and environmental parameters (2008-2018) across riverine, estuarine, and precipitation inputs and outputs. River inputs include the Winnicut (WNC), Lamprey (LMP), and Squamscott (SQR). Estuarine concentrations include Adams Point high tide input (AP HT) and low tide output (AP LT). Concentrations are reported as mean ± standard deviation (n). PN and TSS were assumed to be 0 for precipitation.

Parameter	WNC	LMP	SQR	AP HT	Precipitation	AP LT
PO_4^{3-} (ug P L^{-1})	11.2 ± 7.1 (68)	6.95 ± 4.4 (67)	9.68 ± 6.9 (67)	19.9 ± 11.7 (128)	5.18 ± 5.17 (533)	18.9 ± 11.2 (129)
PN (mg N L^{-1})	0.0572 ± 0.03 (57)	0.0648 ± 0.03 (59)	0.0715 ± 0.05 (61)	0.0745 ± 0.04 (121)	–	0.0989 ± 0.06 (121)
TN (mg N L^{-1})	0.65 ± 0.25 (105)	0.46 ± 0.11 (107)	0.52 ± 0.18 (110)	0.32 ± 0.08 (120)	0.52* ± 0.53 (563)	0.36 ± 0.12 (121)
TDN (mg N L^{-1})	0.51 ± 0.12 (109)	0.35 ± 0.09 (110)	0.39 ± 0.1 (111)	0.25 ± 0.08 (127)	0.52 ± 0.53 (563)	0.27 ± 0.1 (129)
NH_4^+ (ug N L^{-1})	26.4 ± 17.9 (105)	16.3 ± 13.05 (101)	17.3 ± 12.56 (107)	32.9 ± 28.41 (123)	238 ± 317 (562)	32.3 ± 24.59 (125)
$NO_3^- + NO_2^-$ (mg N L^{-1})	0.18 ± 0.12 (106)	0.12 ± 0.06 (107)	0.10 ± 0.05 (108)	0.09 ± 0.06 (128)	0.25† ± 0.24 (560)	0.08 ± 0.06 (129)
DIN (mg N L^{-1})	0.21 ± 0.12 (105)	0.13 ± 0.06 (101)	0.12 ± 0.06 (107)	0.12 ± 0.07 (123)	0.48 ± 0.49 (547)	0.11 ± 0.07 (125)
DON (mg N L^{-1})	0.30 ± 0.1 (105)	0.22 ± 0.08 (101)	0.28 ± 0.09 (107)	0.13 ± 0.05 (122)	0.05 ± 0.12 (541)	0.15 ± 0.08 (125)
DOC (mg C L^{-1})	8.09 ± 2.73 (89)	5.99 ± 1.49 (90)	7.79 ± 1.91 (91)	2.60 ± 0.78 (98)	1.82 ± 3.47 (560)	2.73 ± 0.87 (98)
TSS (mg L^{-1})	4.90 ± 8.95 (107)	2.32 ± 1.22 (107)	3.50 ± 3.99 (111)	15.7 ± 5.71 (117)	–	20.1 ± 10.81 (113)
Temperature (°C)	12.6 ± 7.78 (111)	13.5 ± 8.41 (111)	13.4 ± 8.24 (113)	11.5 ± 7.56 (128)	–	11.6 ± 7.90 (129)
Dissolved Oxygen (%)	80.3 ± 15.16 (111)	86.9 ± 14.37 (111)	79.5 ± 16.25 (113)	98.0 ± 12.27 (128)	–	98.2 ± 9.81 (129)
Dissolved Oxygen (mg/L)	8.98 ± 2.98 (111)	9.52 ± 3.10 (111)	8.80 ± 3.20 (113)	9.64 ± 2.06 (128)	–	9.68 ± 2.18 (129)

*Precipitation TN concentrations were assumed to be equal to TDN concentrations.
†Precipitation is analyzed for NO_3^- but it was assumed to be equal to $NO_3^- + NO_2^-$.

Table 2. Average and standard deviation of annual flow-weighted concentrations for tributaries and precipitation inputs to Great Bay. Wastewater treatment facility concentration is the average of reported monthly concentrations. Adams Point high and low tide concentrations were averaged together to represent an estuarine outflow concentration. Solutes with statistically different mean high and low tide concentrations were not included, except for TN due to its distribution overlap. Concentrations are in mg L^{-1}.

Solute	LMP	SQR	WNC	Precipitation	WWTF**	Estuarine
TN	0.44 ± 0.04	0.46 ± 0.05	0.60 ± 0.08	0.31 ± 0.05*	26.2 ± 6.1	0.34 ± 0.11
PN	0.05 ± 0.01	0.06 ± 0.02	0.05 ± 0.01	–	–	–
DIN	0.13 ± 0.02	0.12 ± 0.02	0.19 ± 0.04	0.28 ± 0.05	–	0.12 ± 0.07
DOC	5.84 ± 0.55	7.32 ± 0.68	7.88 ± 1.32	1.1 ± 0.53	–	2.67 ± 0.83
PO_4^{3-}	0.01 ± 0.003	0.01 ± 0.004	0.01 ± 0.01	0.004 ± 0.001	–	0.02 ± 0.01
TSS	2.54 ± 0.82	3.07 ± 1.31	5.15 ± 5.48	–	–	–

*TDN assumed to equal TN.

**WWTF concentrations are the average of the three treatment facilities average concentration. In years where only load information was available, concentrations were not able to be included in the average concentration calculation. Average TN concentrations by facility are as follows: Exeter (24 mg-N/L ± 7.6); Newmarket (33.1 mg-N/L ± 13); Newfields (21.53 mg-N/L). There is no reported standard deviation for Newfields effluent concentration.

Table 3. Mean annual primary productivity, respiration, and net ecosystem metabolism. Values are averages of the daily integrated values for each year. Net ecosystem metabolism is the difference between primary productivity and ecosystem respiration.

Year (n)	Primary Productivity (mmol O_2 m^{-2} d^{-1})	Respiration (mmol O_2 m^{-2} d^{-1})	Net Ecosystem Metabolism (mmol O_2 m^{-2} d^{-1})
2014 (189)	55.4	-58.4	3.1
2015 (119)	59.2	-55.5	3.7
2016 (218)	61.6	-62.0	-0.4
2017 (227)	89.3	-92.0	-2.6
2018 (166)	152.1	-150.2	1.9

FIGURES

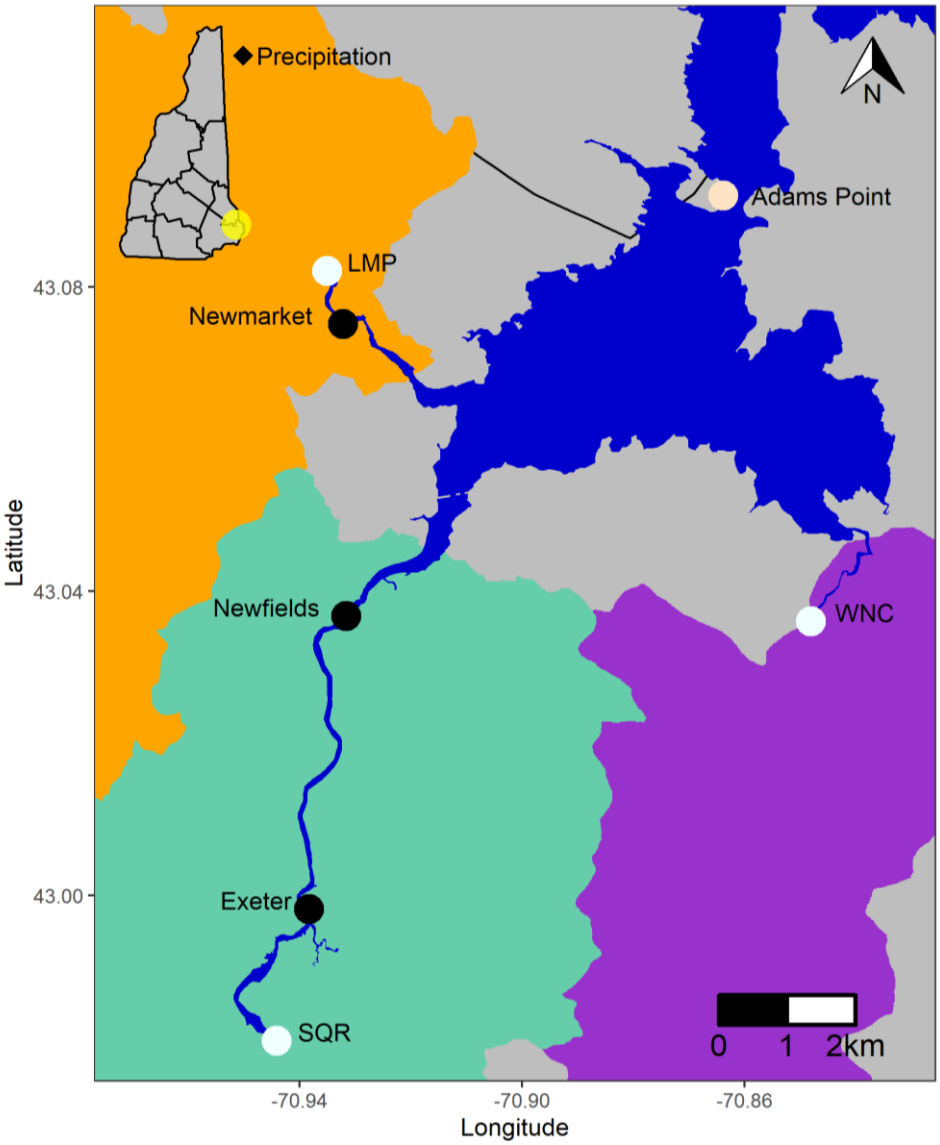

Figure 1. Map of Great Bay and the three major watersheds, the Lamprey (orange), Squamscott (green), and Winnicut (purple) rivers. Long-term tributary water quality monitoring stations are denoted with white circles, wastewater treatment facilities with black circles, and estuarine water quality monitoring with a circle at Adams Point. The location of the wet deposition collector within the Lamprey River watershed is noted (black diamond). Inset shows the location of Great Bay Estuary within the state of New Hampshire. Black lines denote counties.

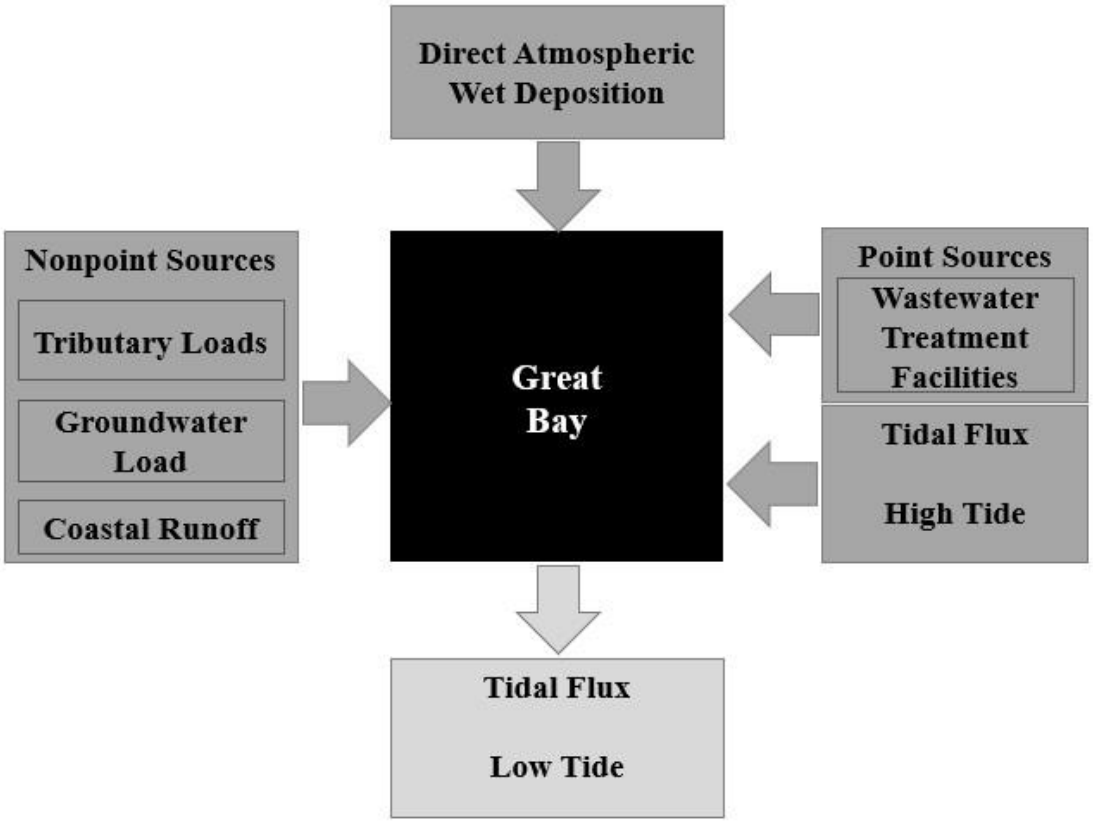

Figure 2. Conceptual model of the solute budget calculated for Great Bay. Inputs to Great Bay were defined as wet deposition, point source wastewater treatment effluent, high tide flux, and nonpoint sources, including tributary watershed loads, groundwater load, and coastal runoff. Output from Great Bay was defined as low tide flux past Adams Point (Figure 1).

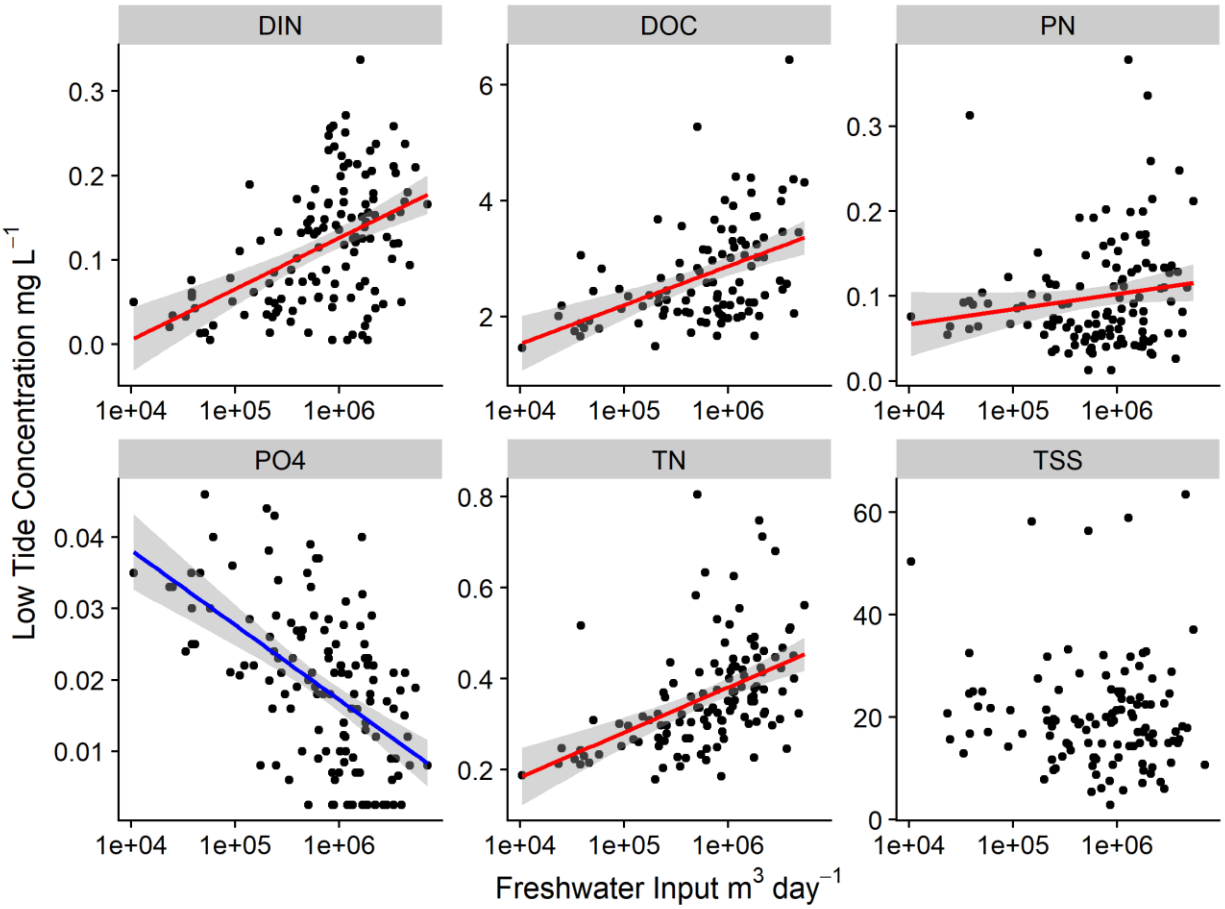

Figure 3. Concentration-discharge relationships at Adams Point during low tide sampling events. Linear regression lines are shown. Blue lines indicate significant ($p < 0.05$) negative slopes and red lines indicate significant ($p < 0.05$) positive slopes. Shading represents standard error.

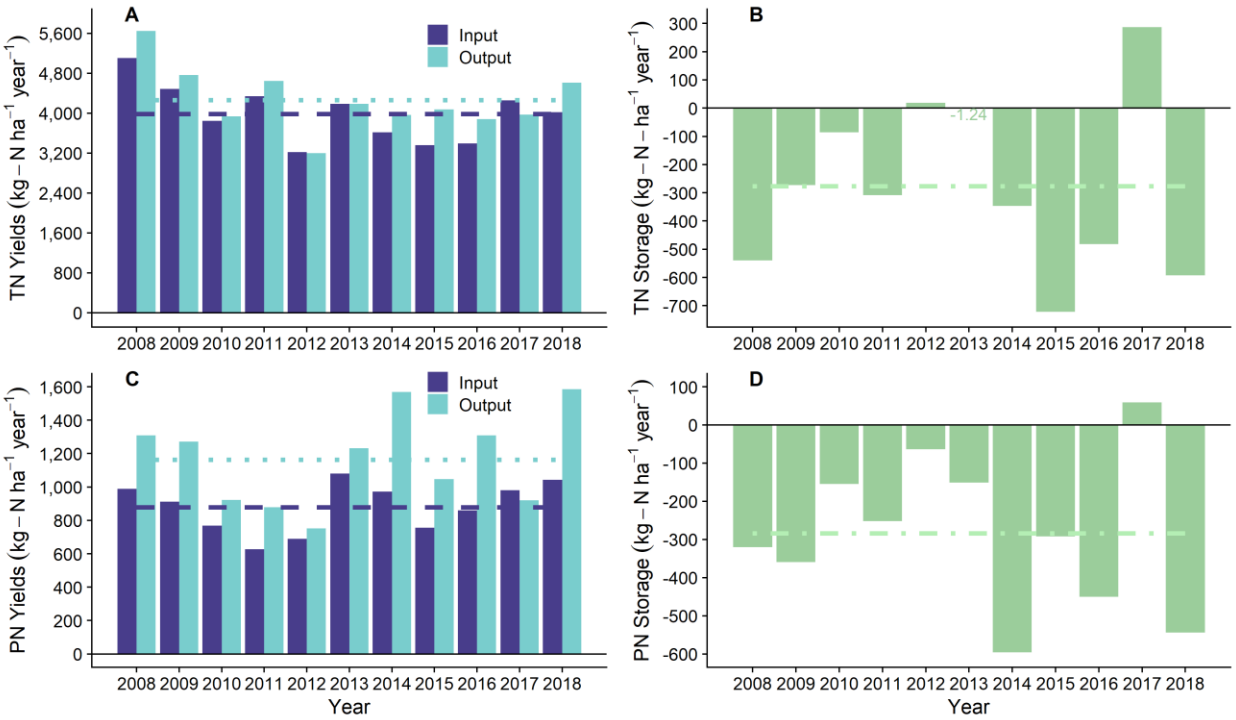

Figure 4. Total nitrogen (TN) and particulate nitrogen (PN) annual input, output, and Δ storage yields (B, D) normalized by Great Bay surface area at mean high tide (kg N ha^{-1} year^{-1}). Dashed lines correspond to the decadal average of input load (purple), output load (blue), and Δ storage (green). TN input loads include watershed sources above the head-of-tide, downstream wastewater treatment point sources, direct wet deposition, groundwater flux, coast runoff, and high tide input into Great Bay (A). PN input loads include watershed sources above the head-of-tide (2013 onward), coastal runoff (2013 onward), and high tide input into Great Bay (C). From 2008 -2012, the black box model only looks at high and low tide flux differences. Output yield is low tide flux out of Great Bay for both solutes.

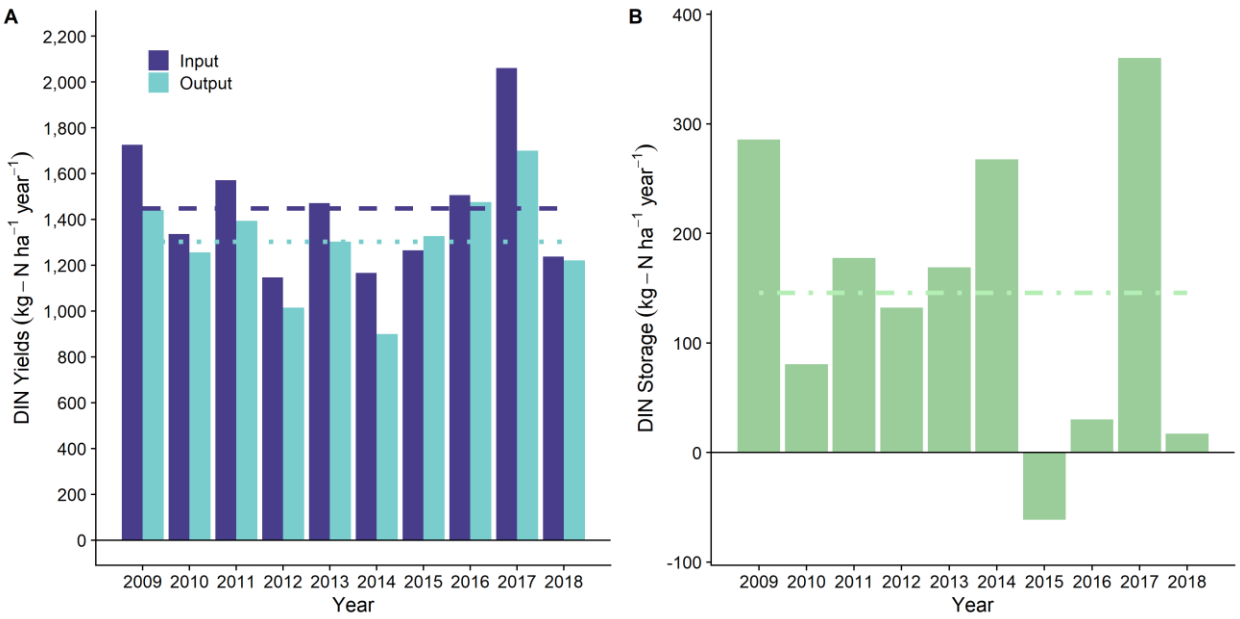

Figure 5. Dissolved Inorganic Nitrogen (DIN) inputs and output (A), and Δ storage (B), normalized by Great Bay surface area at mean high tide (kg N ha^{-1} year^{-1}). Dashed lines correspond to the decadal average of input (purple), output (blue), and Δ storage (green) yields.

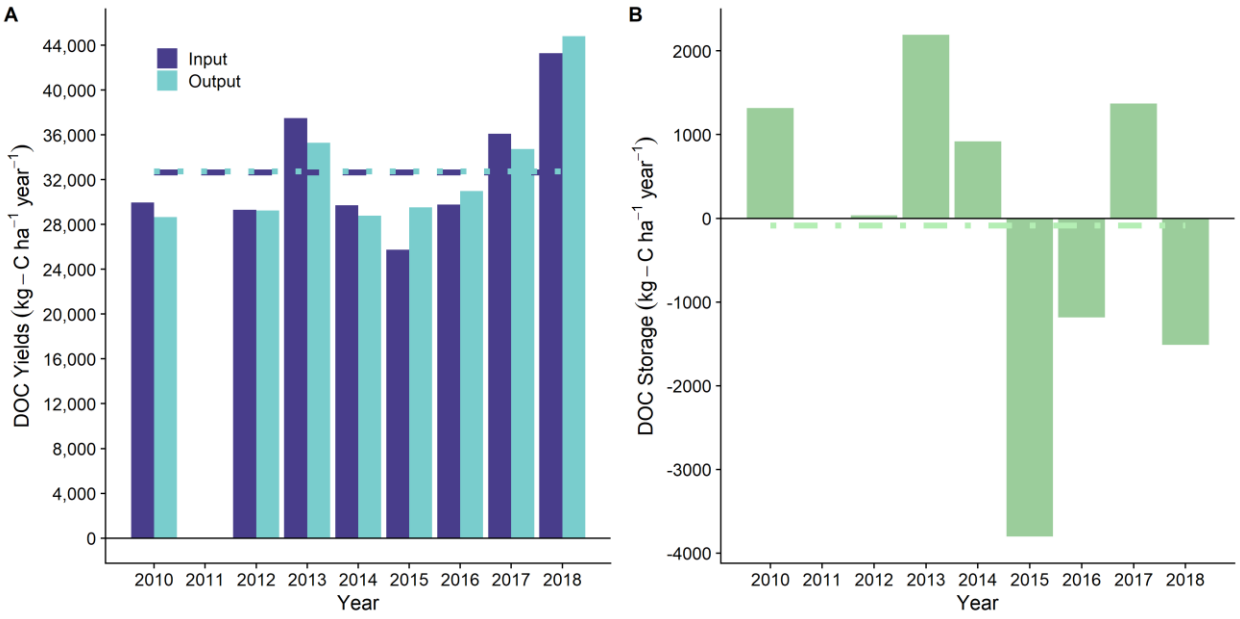

Figure 6. Dissolved organic carbon (DOC) inputs and output (A), and Δ storage (B), normalized by Great Bay surface area at mean high tide (kg C ha^{-1} year^{-1}). Dashed lines correspond to the annual average (n=8) of input load (purple), output load (blue), and Δ storage (green). Input loads include watershed sources above the head-of-tide, wet deposition, coastal runoff, wastewater treatment effluent, and high tide input into Great Bay. Output load is low tide flux out of Great Bay.

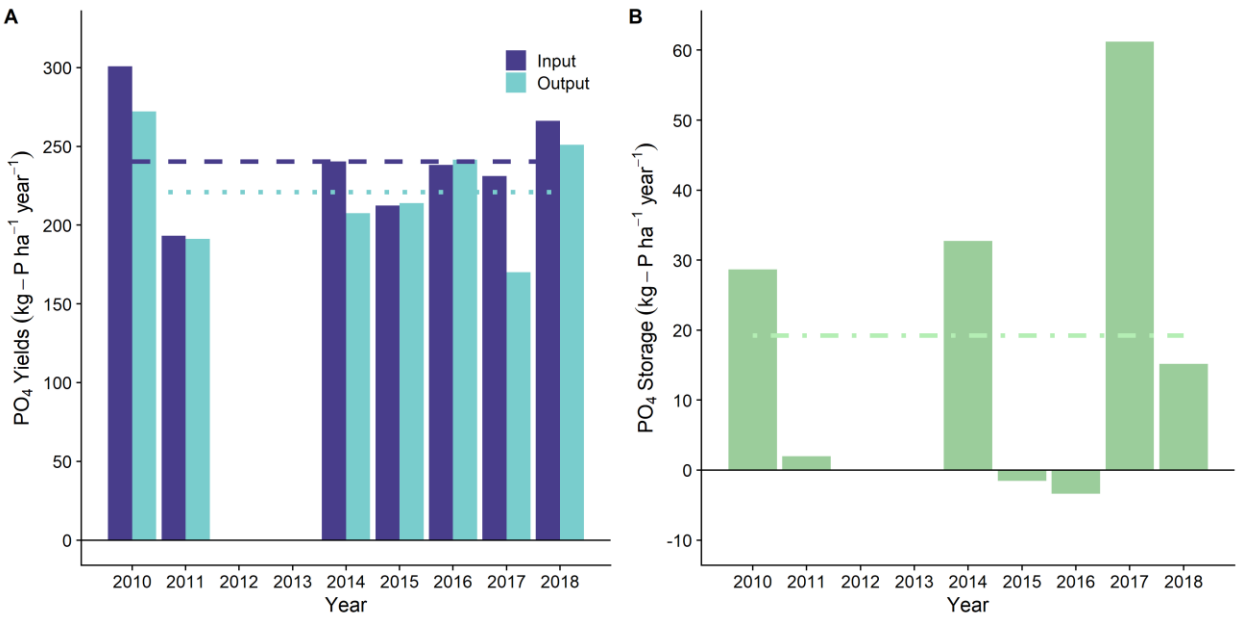

Figure 7. Orthophosphate (PO_4) inputs and output (A), and Δ storage (B), normalized by Great Bay surface area at mean high tide (kg P ha^{-1} $year^{-1}$). Dashed lines correspond to the annual average (n=7) of input yield (purple), output yield (blue), and Δ storage (green). Input loads include watershed sources above the head-of-tide, wet deposition, coastal runoff, wastewater treatment effluent, and high tide input into Great Bay. Output load is low tide flux out of Great Bay. There was insufficient input orthophosphate data in 2012 and 2013.

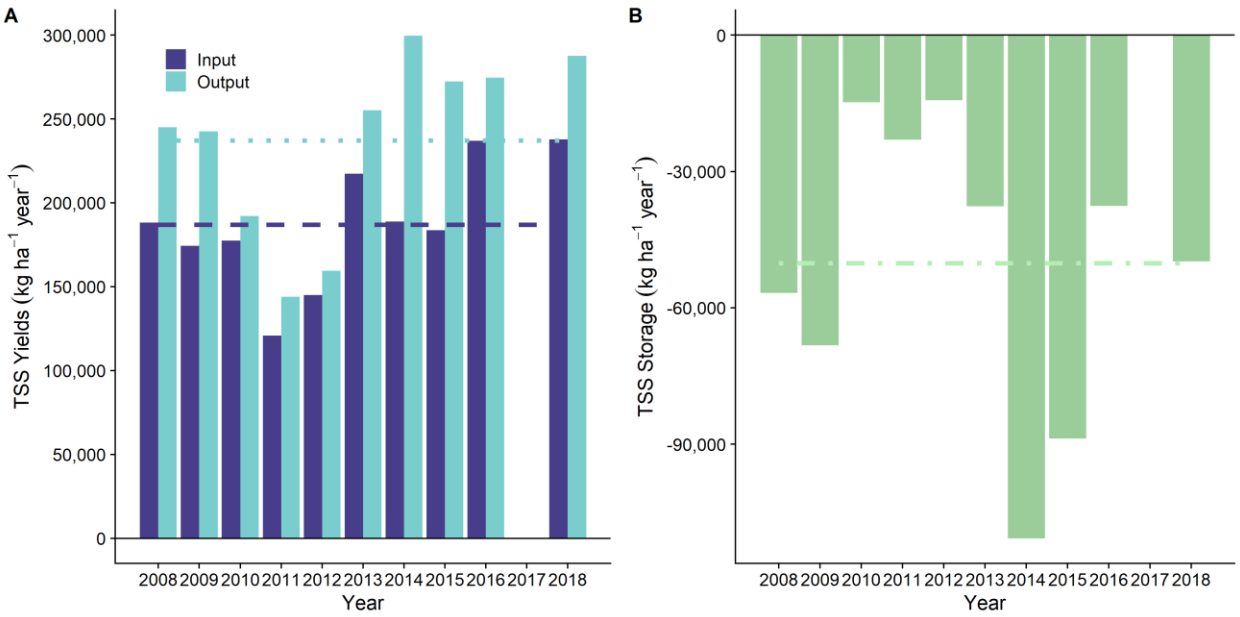

Figure 8. Total suspended solids (TSS) inputs and output (A) and storage (B), normalized by Great Bay surface area at mean high tide (kg ha^{-1} year^{-1}). Dashed lines correspond to the annual average (n=11) of input (purple), output (blue), and Δ storage yield (green). Input loads include watershed sources above the head-of-tide, coastal runoff, wastewater treatment effluent, and high tide input into Great Bay. Output load is low tide flux out of Great Bay. A mass balance in 2017 was not possible due to lack of data.

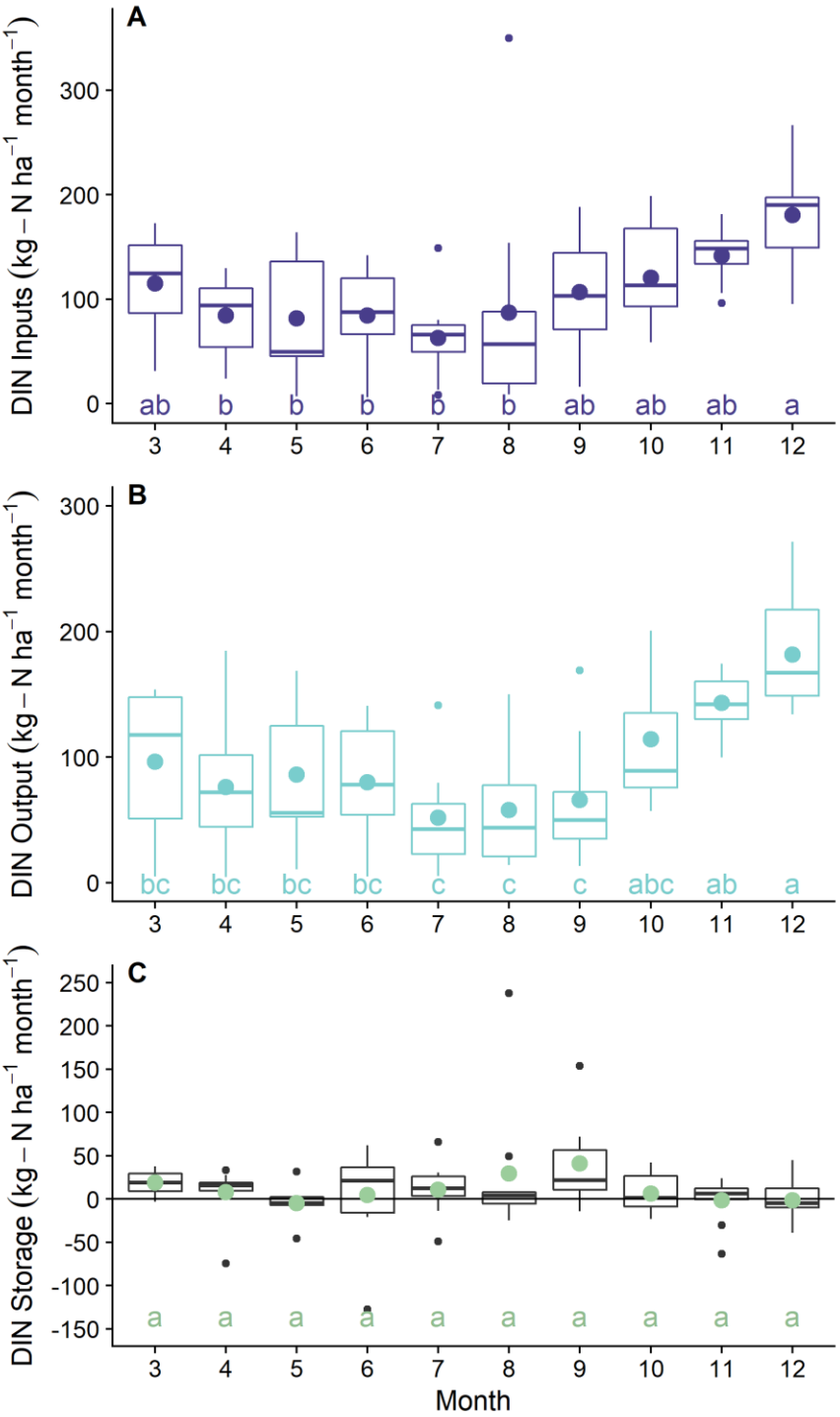

Figure 9. Box and whisker plots of monthly dissolved inorganic nitrogen (DIN) inputs (A), output (B), and storage (C). Bolded circles represent monthly means. Lowercase letters represent results of post hoc Tukey test, months sharing the same letter(s) are not significantly different ($p > 0.05$).

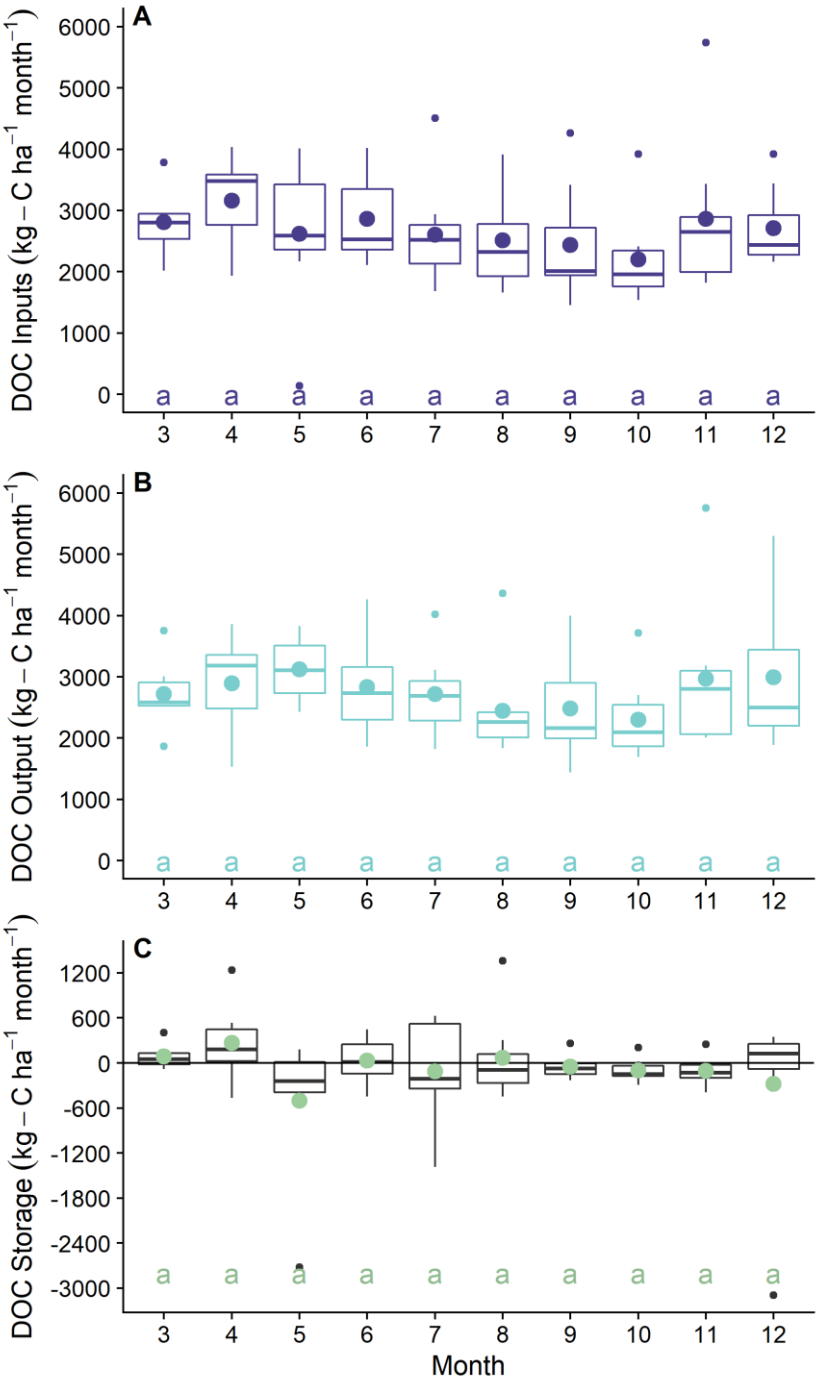

Figure 10. Box and whisker plots of monthly dissolved organic carbon (DOC) inputs (A), output (B) and storage (C). Bolded circles represent monthly means. There was no significant difference between months across inputs, output, and Δ storage of DOC. Lowercase letters represent results of post hoc Tukey test, months sharing the same letter(s) are not significantly different ($p > 0.05$).

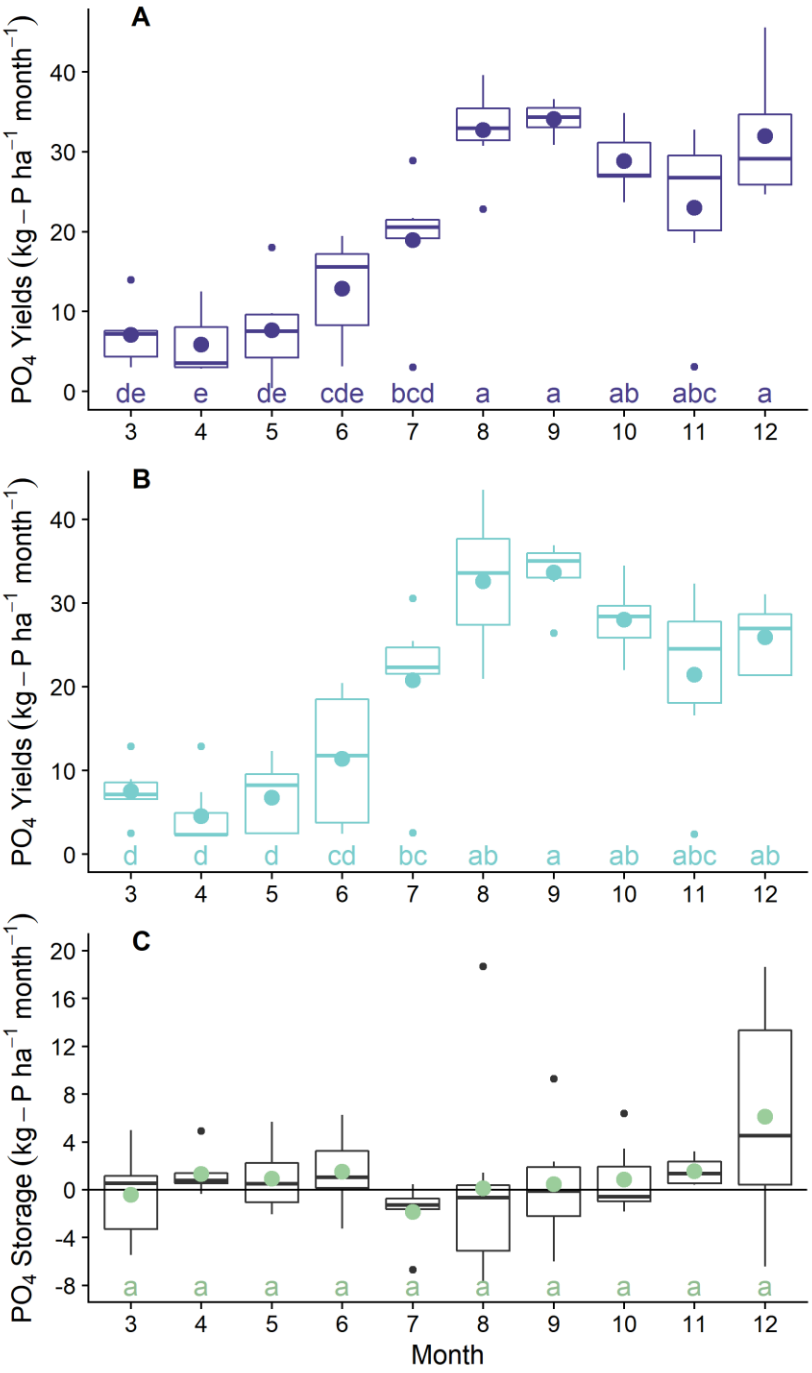

Figure 11. Box and whisker plots of monthly orthophosphate inputs (A), output (B), and storage (C). Bolded circles represent monthly means. Lowercase letters represent results of post hoc Tukey test, months sharing the same letter(s) are not significantly different ($p > 0.05$).

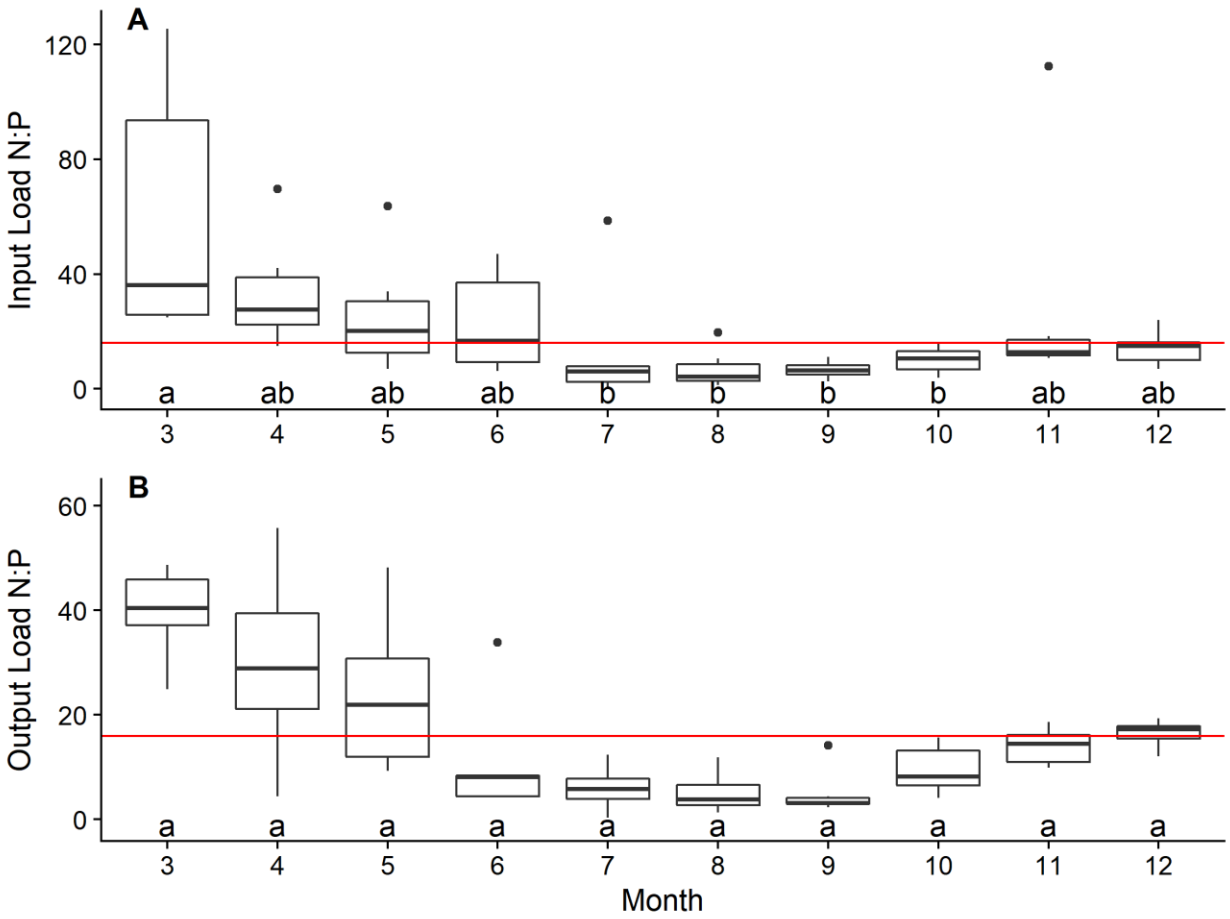

Figure 12. Box and whisker plot of molar DIN:PO_4^{3-} ratios for monthly inputs (A) and outputs (B) in the Great Bay box model. Red line indicates Redfield's Ratio of 16:1.

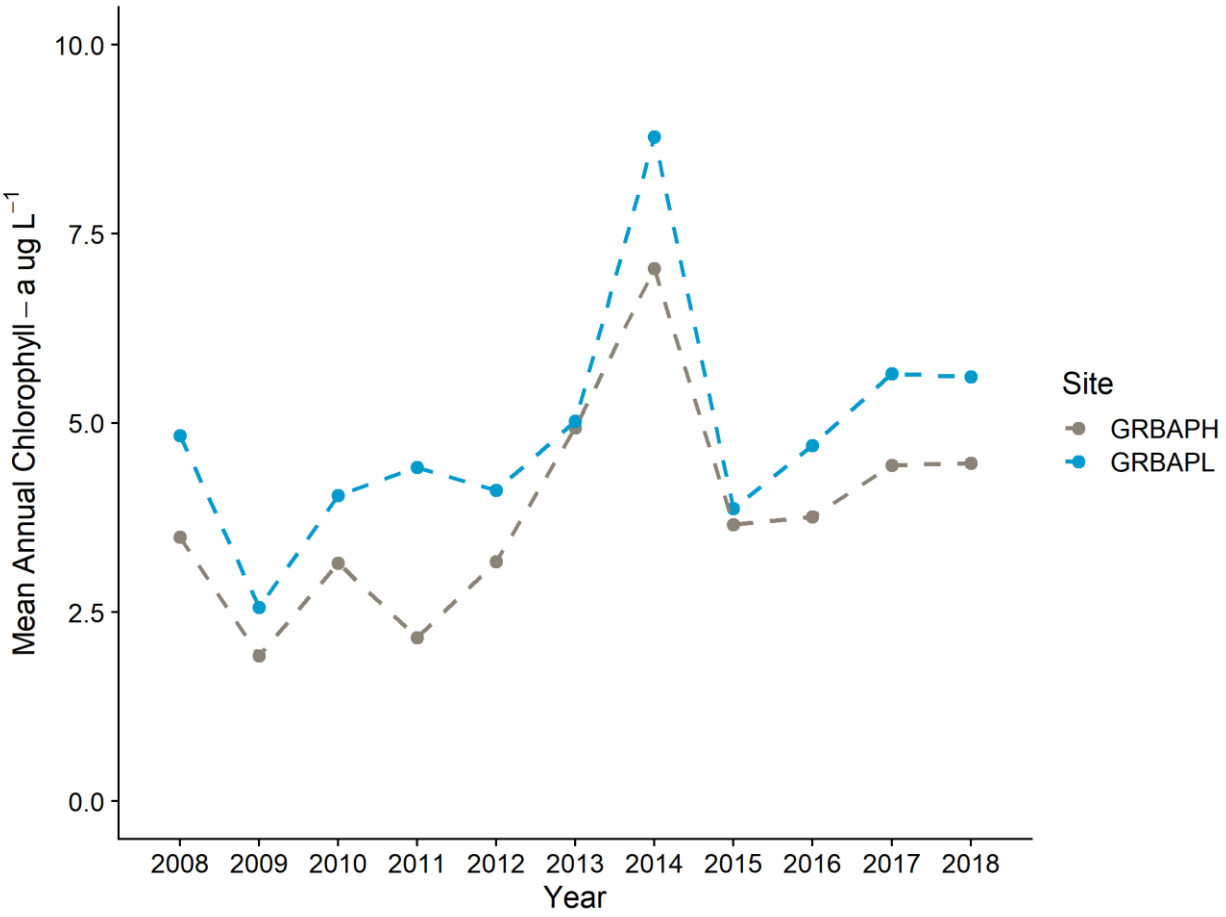

Figure 13. Annual average chlorophyll-a concentrations over time at Adams Point during high tide (grey) and low tide (blue). Annual averages represent the mean of monthly concentrations (n=12).

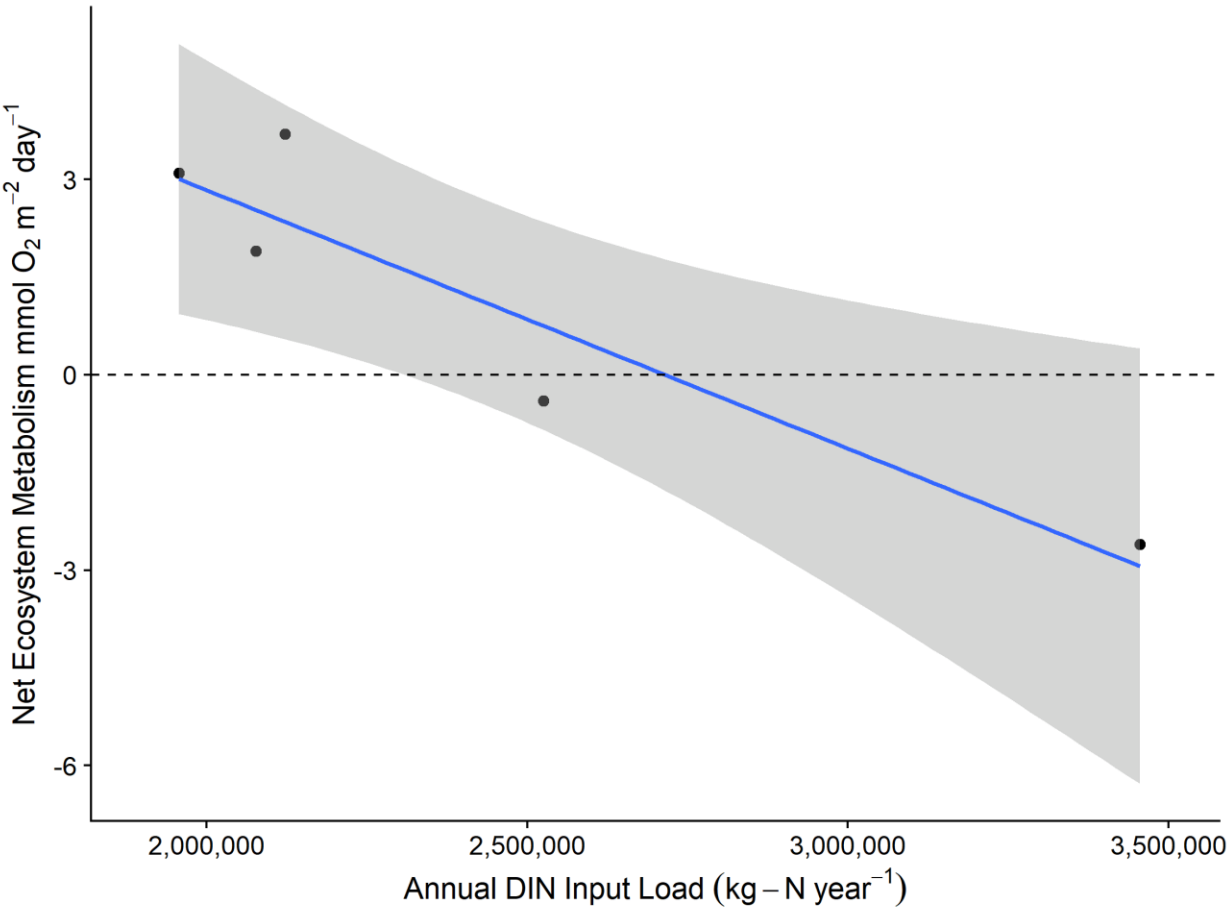

Figure 14. Linear regression between annual dissolved inorganic nitrogen (DIN) input loads to Great Bay and net ecosystem metabolism ($r^2 = 0.8212$, $p < 0.05$, n=5). Data was only available between 2014 and 2018. Blue line represents the regression line and grey area represents the 95% confidence interval.

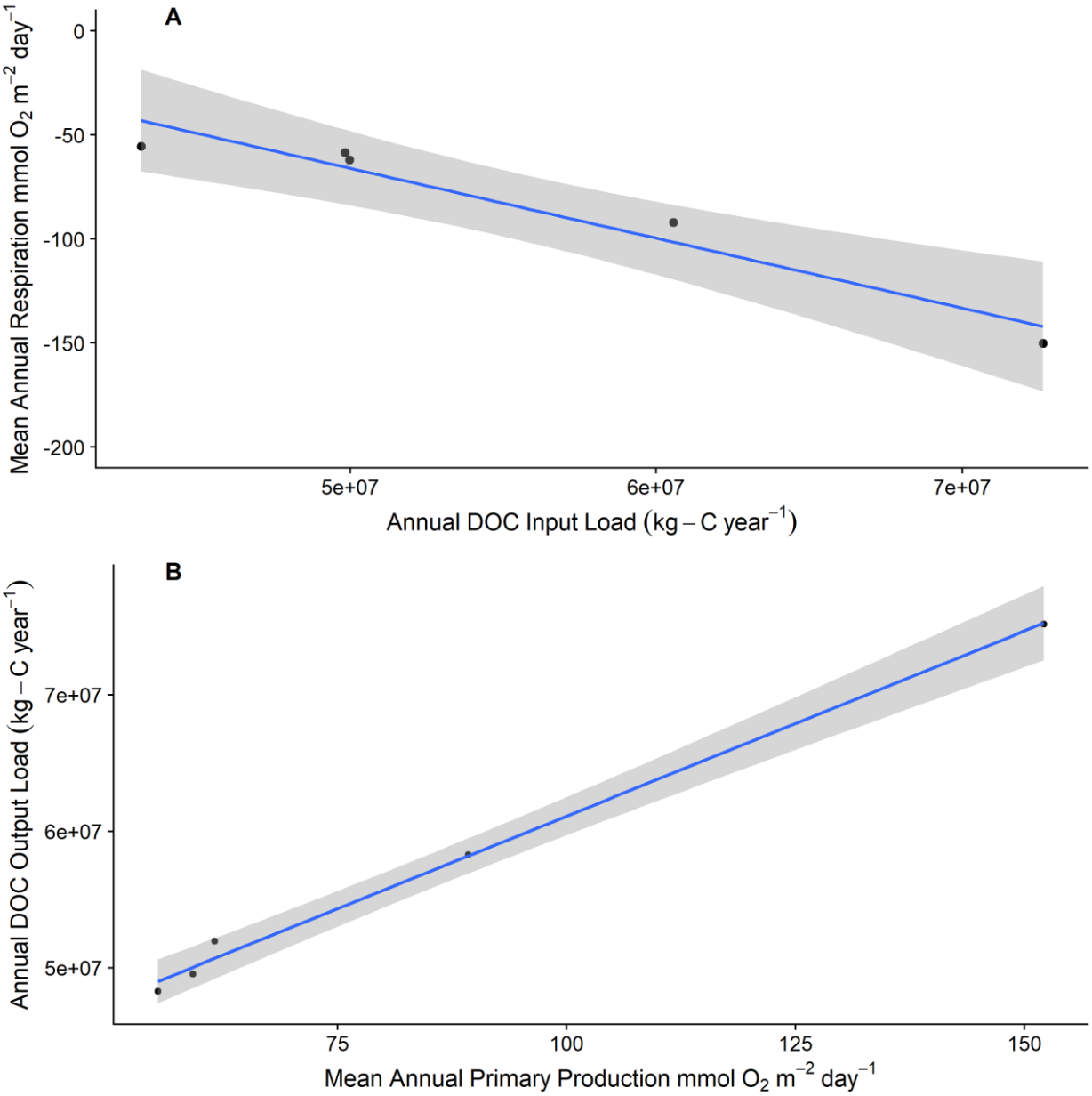

Figure 15. Linear regression between annual dissolved organic carbon (DOC) input loads to Great Bay and mean annual respiration rates (r^2 = 0.9216, $p < 0.05$, n=5) (A) and linear regression between mean annual primary production and annual DOC output loads (r^2 = 0.9935, $p < 0.05$, n=5) (B). Data was only available between 2014 and 2018. Linear regression percent error is 10.99% (A) and 2.63% (B). Blue line represents the regression line and grey area represents the 95% confidence interval.

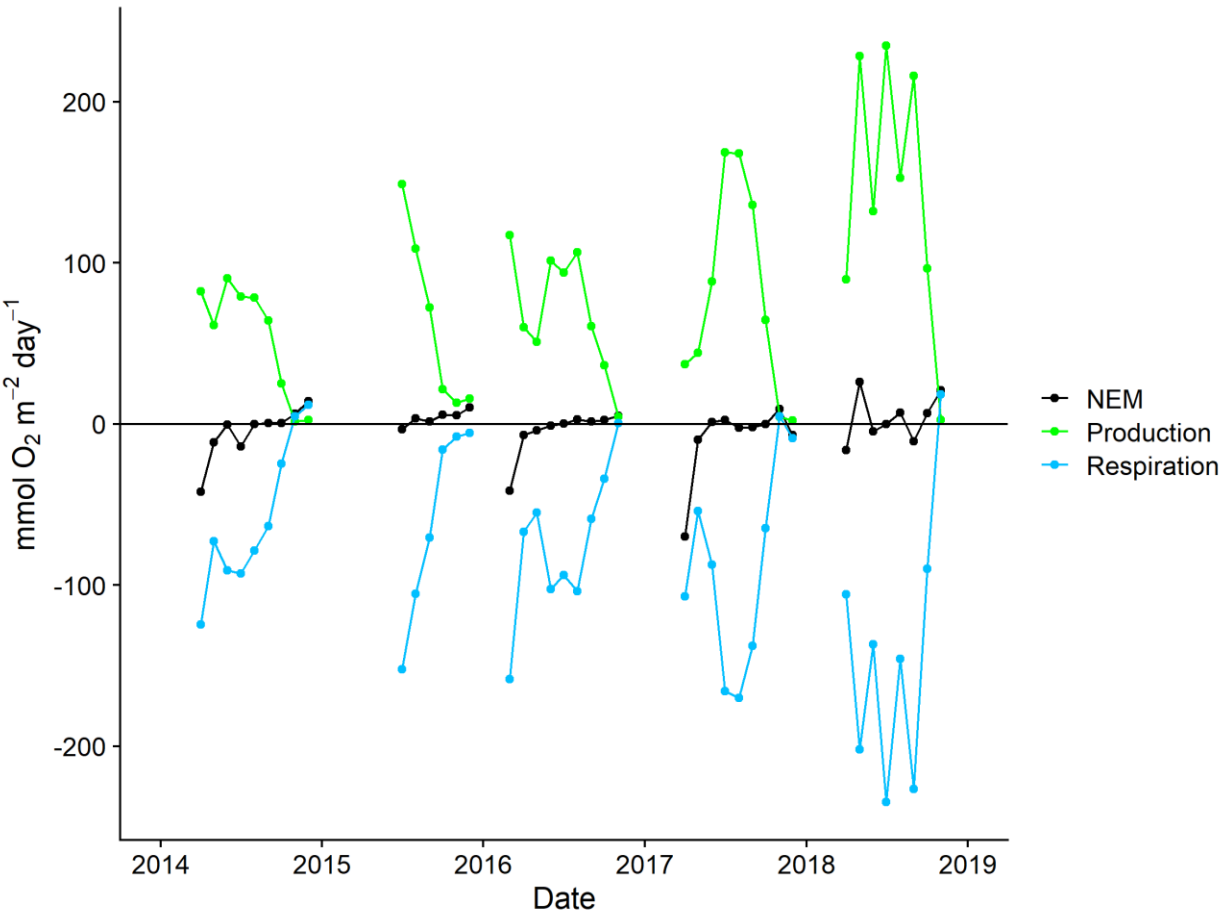

Figure 16. Monthly net ecosystem metabolism (black), production (green) and respiration (blue) rates over time.

APPENDICES

Appendix A: Supplemental Data Tables

Table A1. Flow multipliers for discharge estimates (Piscataqua Region Estuaries Partnership, 2012).

Tributary (USGS Gage Number)	Watershed Area (ha)	Stream Gauge Watershed Area	Flow Multiplier
Lamprey (01073500)	54897.39	47914.78	1.14573
Squamscott (01073587)	27686.97	16446.42	1.683529
Winnicut (01073785)	3672.60	3651.88	1.005443

Table A2. Wastewater treatment facility (WWTF) annual (CY) solute loads for TN, TSS, and DIN, DOC, and PO_4. Newmarket loads between 2008 and 2011 were estimated from the PREP 2012 Environmental Data Report. 2012 and 2013 Newmarket loads are the reported average from the *State of Our Estuaries* report (2018). Exeter loads were sourced from the Town of Exeter (Town of Exeter, 2019).

WWTF	Year	TN (kg-N/year)	TSS (kg/year)	DIN (kg-N/year)	DOC (kg-C/year)	PO_4 (kg-P/year)
Exeter	2008	38737	43717	32539	36680	4146
Exeter	2009	37920	40173	31853	35907	4059
Exeter	2010	37920	50732	31853	35907	4059
Exeter	2011	37920	73263	31853	35907	4059
Exeter	2012	39083	52949	32830	37008	4183
Exeter	2013	50338	45469	42284	47665	5388
Exeter	2014	43700	45171	36708	41380	4677
Exeter	2015	51419	47877	43192	48689	5503
Exeter	2016	47926	55107	40258	45381	5130
Exeter	2017	62807	60031	52758	59472	6722
Exeter	2018	56121	56131	47141	53141	6007
Exeter	2019	39665	33264	33318	37559	4245
Newfields	2008	2896	998	2432	1531	310
Newfields	2009	2739	1335	2301	1448	293
Newfields	2010	2683	1004	2254	1418	287
Newfields	2011	2874	1888	2414	1519	308
Newfields	2012	2576	2154	2164	1362	276
Newfields	2013	2726	888	2290	1441	292
Newfields	2014	2701	644	2269	1428	289
Newfields	2015	2684	533	2255	1419	287
Newfields	2016	2619	851	2200	1384	280
Newfields	2017	2713	1701	2279	1434	290
Newfields	2018	2759	1124	2318	1458	295
Newfields	2019	2653	628	2228	1402	284
Newmarket	2008	27990	15501	23512	19705	2996
Newmarket	2009	27990	15341	23512	19705	2996
Newmarket	2010	27990	16116	23512	19705	2996
Newmarket	2011	27990	17977	23512	19705	2996
Newmarket	2012	31100	15352	26124	21895	3329
Newmarket	2013	31100	18303	26124	21895	3329
Newmarket	2014	29732	19399	24974	20931	3182
Newmarket	2015	24657	14046	20712	17359	2639
Newmarket	2016	28881	18138	24260	20333	3091
Newmarket	2017	16497	14893	13857	11614	1766
Newmarket	2018	3277	3573	2753	2307	351
Newmarket	2019	3966	2072	3331	2792	424

Table A3. Mean annual solute loads (kg year^{-1}) for each calculated, mass balance budget component.

Site	PO4	TN	PN	TDN	NH4	NO3_NO2	DIN	DON	DOC	TSS
AP HT	395568	6354368	1462125	4906380	640043	1680129	2290094	2480944	51718531	3.12E+14
AP LT	374861	7148866	1951522	5251622	627480	1608700	2185601	2851500	54945829	3.98E+14
LMP	2075	140988	15136	106935	5004	34637	39933	60295	1728879	799965
SQR	1540	78098	7424	60573	2716	16016	19046	39102	1111275	533968
WNC	268	15112	1014	11854	500	4065	4534	6762	176829	139694
Exeter	4848	45296	–	–	–	–	38049	–	42891	50324
WWTF Newmarket	2508	23431	–	–	–	–	19682	–	16495	14226
WWTF Newfields	291	2719	–	–	–	–	2284	–	1437	1146
WWTF Precipitation	82	6396	–	6396	2572	3211	5715	706	22760	NA
Coastal Runoff	140	9502	1020	7207	353	2473	2844	4430	116524	53916

Table A4. Range in uncertainty in Δ storage terms for total nitrogen (TN), dissolved inorganic nitrogen (DIN), dissolved organic carbon (DOC), and orthophosphate (PO_4^{3-}). Range was calculated as the difference between high inputs and low outputs and the difference between low inputs and high outputs. Wastewater treatment, groundwater, and runoff terms were held constant.

Solute	Uncertainty Range of Δ Storage Term (kg $year^{-1}$)	Uncertainty Range of Δ Storage Term (kg ha^{-1} $year^{-1}$)
TN	$-4.5x10^6 – 3.5x10^6$	-2,700 – 2,100
DIN	$-2.5x10^6 – 3.1x10^6$	-1,500 – 1,900
DOC	$-3.2x10^7 – 3.4x10^7$	-19,000 – 20,000
PO_4^{3-}	$-4.2x10^5 – 4.9x10^5$	-250 - 290

Appendix B: Supplemental Figures

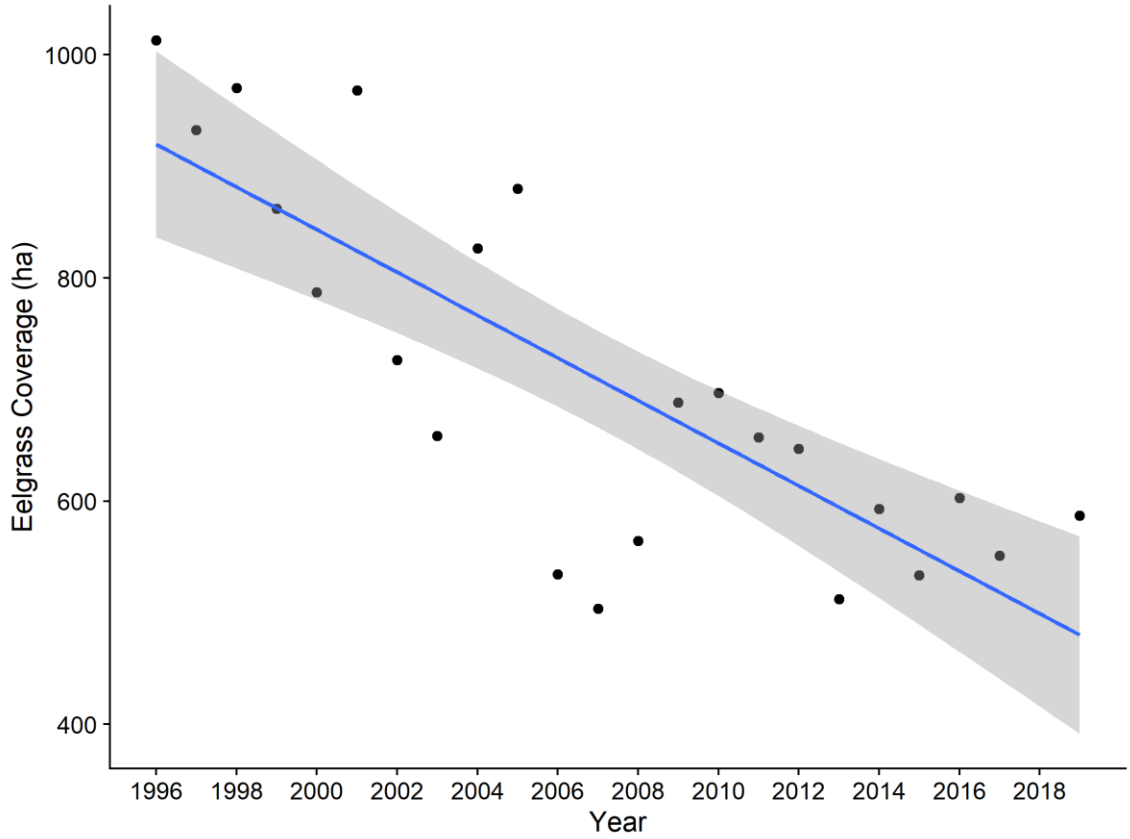

Figure B1. Scatterplot of hectares of eelgrass over time in Great Bay. A strong, negative correlation was found between time and eelgrass coverage ($p < 0.05$, $r = -0.802$). Regression showed that ~63% of the variability in eelgrass coverage can be explained by time ($p < 0.05$, $n=23$). Data sourced from Piscataqua Region Estuaries Partnership Reports 354, 407, 438 (https://scholars.unh.edu/prep)

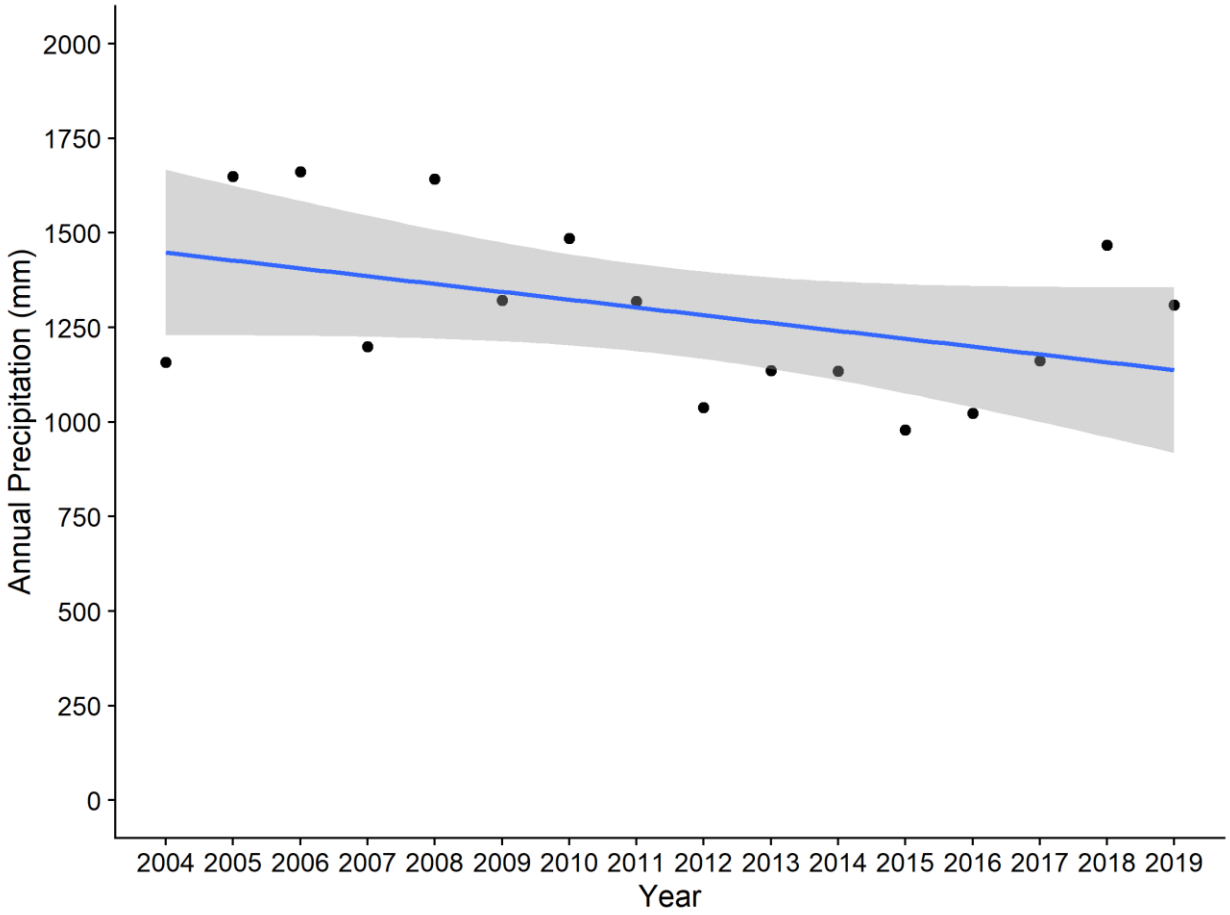

Figure B2. Linear regression between annual precipitation total and time (r^2 = 0.1851, $p < 0.05$, n=16) shows a decrease in rainfall in recent years.

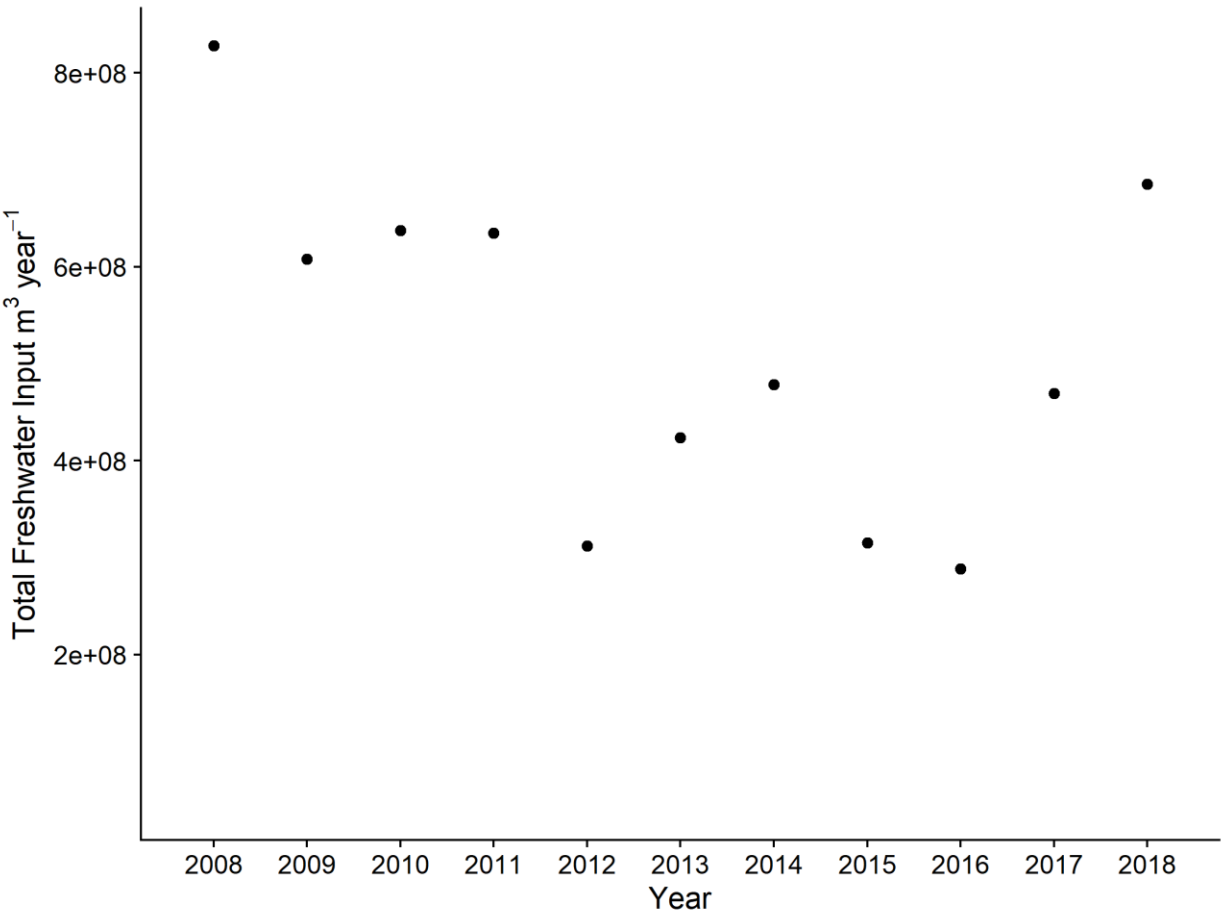

Figure B3. Total freshwater input from the three tidal tributaries of Great Bay over time. Freshwater input did not exhibit a significant trend over time, but low flow years can be seen between 2012 and 2016.

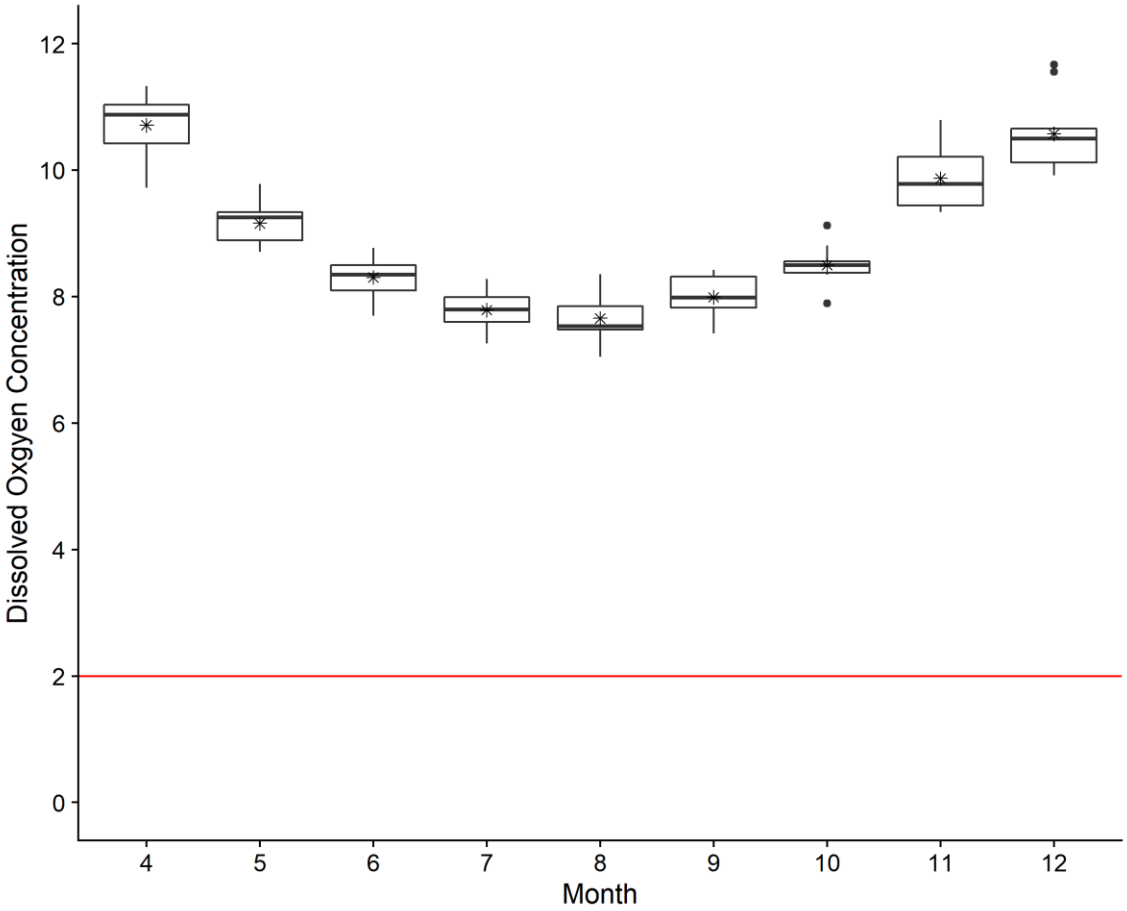

Figure B4. Box and whisker plot of monthly average dissolved oxygen concentrations (mg L^{-1}) between 2008 and 2018. Red line indicates dissolved oxygen concentration under which hypoxia events occur (2 mg L^{-1}).

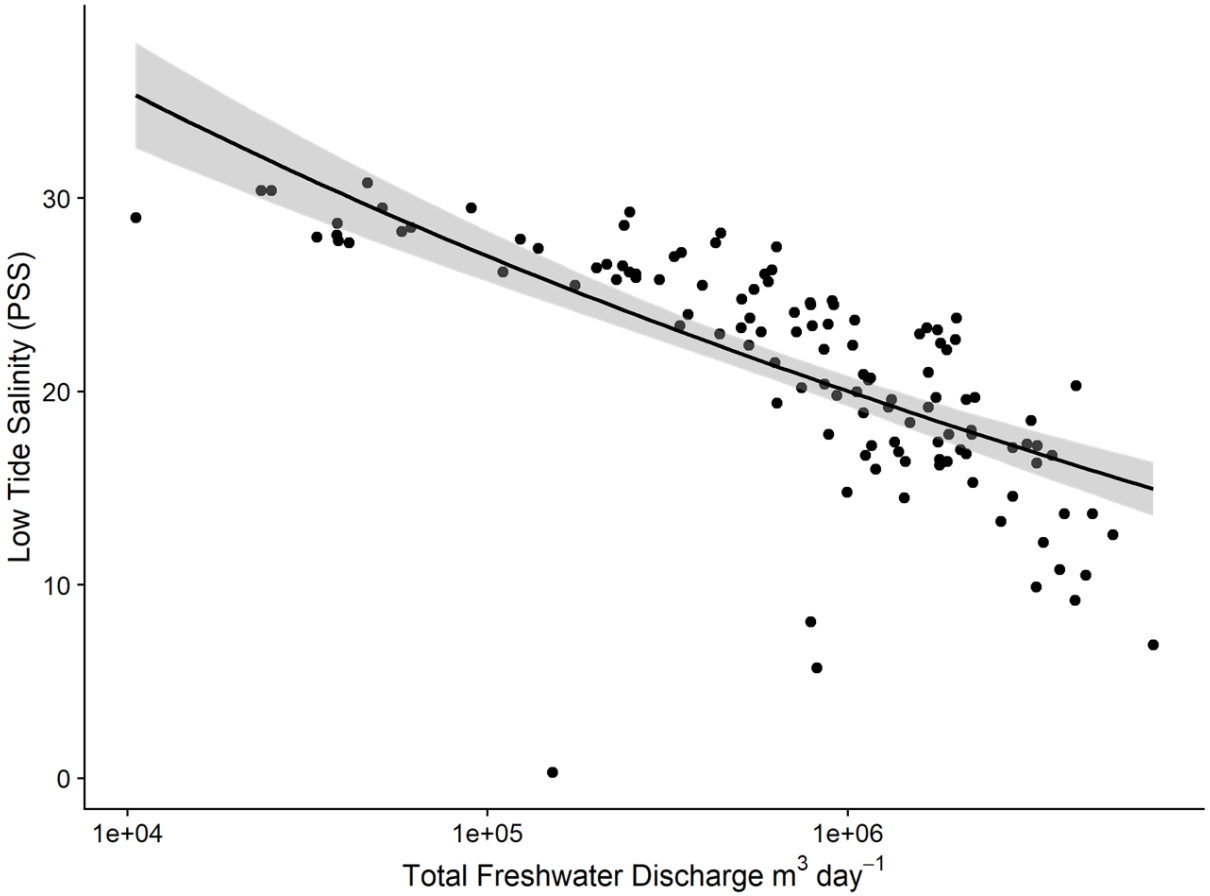

Figure B5. Scatter plot of total, daily, freshwater discharge to Great Bay versus low tide salinity levels. The log-linear regression line and confidence interval is shown (R^2=0.50, $p<0.05$).